Electronic Supplementary Material (ESI) for Journal of Materials Chemistry A.

A Metal–Covalent Organic Framework Catalyst with Pincer Coordination Units for Boosting Transfer Hydrogenation of Quinolines with Ammonia Borane

Wenying Ai[1]*, Xiao Du[1], Yu Yang[1], Zelin Zheng[1], Lipeng Zhai[1], Baiwei Ma[1], Siwen Cui[1], Pengyu Li[1], Liwei Mi[1]*, and Lingbo Qu[2]*

[1]Henan Key Laboratory of Functional Salt Materials, Center for Advanced Materials Research, School of Material and Chemical Engineering, Zhongyuan University of Technology, Zhengzhou 450007 (P. R. China)

[2]College of Chemistry, and Institute of Green Catalysis, Zhengzhou University, 100 Science Avenue, Zhengzhou, Henan Province 450001, People's Republic of China

Contents

Section A. Materials and Methods

Nuclear magnetic resonance spectra (^{1}H NMR and ^{13}C NMR) were measured on a Bruker 400 MHz spectrometer. The chemical shifts were reported in ppm referenced to the deuterated solvents. Solid state Fourier ^{13}C NMR spectra were measured on a Bruker 400 MHz spectrometer. X-ray diffraction (XRD) data were performed on a Bruker D8 Focus Powder X-ray Diffractometer by using powder on glass substrate, from $2\theta = 2°$ up to 30° with 0.01° increment. Fourier transform infrared (FT IR) spectra were recorded on a JASCO model FT IR-6100 infrared spectrometer. TGA measurements were recorded on a Discovery TGA under N_2, by heating from 30 to 800 °C at a rate of 10 °C min^{-1}. Elemental analysis was performed on an Elementar vario MICRO cube elemental analyzer. Nitrogen sorption isotherms were measured at 77 K with a TriStar II instrument (Micromeritics). The Brunauer-Emmett-Teller (BET) method was utilized to calculate the specific surface areas. By using the non-local density functional theory (NLDFT) model, the pore volume was derived from the sorption curve. Morphology images were characterized with a Zeiss Merlin Compact filed emission scanning electron microscope (FE-SEM) equipped with an energy-dispersive X-ray spectroscopy (EDS) system at an electric voltage of 5 KV. ICP-MS was carried out on a Perkin-Elmer Elan DRC II quadrupole inductively coupled plasma mass spectrometer analyzer. X-ray photoelectron spectroscopy (XPS) experiments were performed on a Thermo Scientific K-Alpha XPS spectrometer using an AlKa X-ray radiation source.

Simulations. The process of simulating COF structure was accomplished via Materials Studio software (version 8.0) of Accelrys Company. The hexagonal crystal system with P6 symmetry group was set as the initial AA stacking COFs structures. The cell parameters a and c were obtained from the calculation of experimental PXRD of COF by Bragg's law. After the smallest asymmetric unit was filled into the blank cell, the Forcite tools package was employed to optimize the cell geometry including energy minimization. The AB stacking structure was built with the similar process as described above, with the exception that a supercell with double c value was selected as the initial

cell of staggered structure. The cell optimized from the universal force fields was subsequently refined using the Pawley refinement method in Reflex tools.[S1-S3]

Computational calculations: The crystalline structure of BIPY-COF was determined using the density-functional tight-binding (DFTB+) method including Lennard-Jones (LJ) dispersion. The calculations were carried out with the DFTB+ program package version 1.2. DFTB is an approximate density functional theory method based on the tight binding approach and utilizes an optimized minimal LCAO Slater-type all-valence basis set in combination with a two-center approximation for Hamiltonian matrix elements. The Coulombic interaction between partial atomic charges was determined using the self-consistent charge (SCC) formalism. Lennard-Jones type dispersion was employed in all calculations to describe vander Waals (vdW) and π-stacking interactions. The lattice dimensions were optimized simultaneously with the geometry. Standard DFTB parameters for X–Y element pair (X, Y = C, H, N) interactions were employed from the mio-0-1 set.

Pawley refinement: Molecular modeling and Pawley refinement were carried out using Reflex, a software package for crystal determination from XRD pattern, implemented in MS modeling version 4.4 (Accelrys Inc.). Initially, unit cell dimensions for both hexagonal and rhombic lattices were taken from the DFTB calculation and the space group for hexagonal and rhombic crystal system were selected as P6, respectively. Pawley refinement was performed for hexagonal S4 lattice to optimize the lattice parameters iteratively until the RWP value converges. The pseudo Voigt profile function was used for whole profile fitting and Berrar–Baldinozzi function was used for asymmetry correction during the refinement processes.

Stability test. The bipy-COF sample (20 mg) was kept at room temperature for 24 h in HCl (1 M), and NaOH (1 M), respectively. The samples were collected by filtration and rinsed with water (30×3 mL) and THF/MeOH(1:1, 30×3 mL). The sample was dried at 100 °C under vacuum overnight and subjected to PXRD.

Section B. Synthetic Procedures

2,6-Pyridine dialdehyde **1**, 1,3,5-Tris(4-aminophenyl)benzene **2**, AcOH, *n*-Butanol (BuOH) and 1,2-Dichlorobenzene (*o*-DCB) were purchased from Heowns. All the other solvents were purchased from Heowns and used as received without further purification.

Synthesis of bipy-COF. The synthesis of bipy-COF was carried out via Schiff-base condensation of 2,6-pyridine dialdehyde **1** (30.4 mg, 0.225 mmol) and 1,3,5-tris(4-aminophenyl)benzene **2** (52.6 mg, 0.15 mmol) in DCB:*n*-butanol (1.5mL, 1:1) using 6 M AcOH aqueous (0.15 mL). Then the suspension was sonicated and heated at 120 °C for 3 days using glass ampule. The resulting precipitate was washed with THF (3×10 mL) and MeOH (3×10 mL), and dried under vacuum overnight to generate bipy-COF as a tawny powder in 93% yield.

Synthesis of Ni-bipy-COF. Nickel acetate (25 mg) was dissolved in 20 mL of MeOH, and then bipy-COF (399.5 mg) was added. The mixture was stirred at room temperature for 48 h. The resulting precipitate was collected by centrifugation, washed with 0.5 M HCl (3×10 mL), H_2O (3×10 mL), and MeOH (3×10 mL), respectively, and then dried under vacuum at 75 °C overnight to give Ni-bipy-COF in 97% yield. The Ni content was 0.98 wt% as determined by ICP-MS.

General Procedure for the Optimization of Reaction Conditions for the Ni-bipy-COF-catalyzed Transfer Hydrogenation of Quinoline.

To a mixture of ammonia borane (15 mg, 0.4873 mmol, 5.0 equiv), Ni-bipy-COF (5 mg) and *n*-hexane (1 mL) in a 25 mL sealed glass tube were added quinoline (0.09747 mmol, 1.0 equiv). The reaction was stirred at 90 °C for 2 h. Then, the mixture was cooled to room temperature, and extracted with EtOAc. The organic layer was washed with brine (30 mL) and dried over Na_2SO_4. The solvent was removed under vacuum and the crude material was purified by column chromatography (EtOAc/petroleum ether) to afford 1,2,3,4-tetrahydroquinoline.

General Procedure for the Transfer Hydrogenation of Quinolines.

To a mixture of ammonia borane (154 mg, 5 mmol, 5.0 equiv), Ni-bipy-COF (50 mg) and *n*-hexane (10 mL) in a 50 mL sealed glass tube were added quinolines (1 mmol, 1.0 equiv). The reaction was stirred at 90 °C for 2 h. Then, the mixture was cooled to room temperature, and extracted with EtOAc. The organic layer was washed with brine (300 mL) and dried over Na_2SO_4. The solvent was removed under vacuum and the crude material was purified by column chromatography (EtOAc/petroleum ether) to afford 1,2,3,4-tetrahydroquinolines in 98-62% yield.

Section C. Supporting Figures

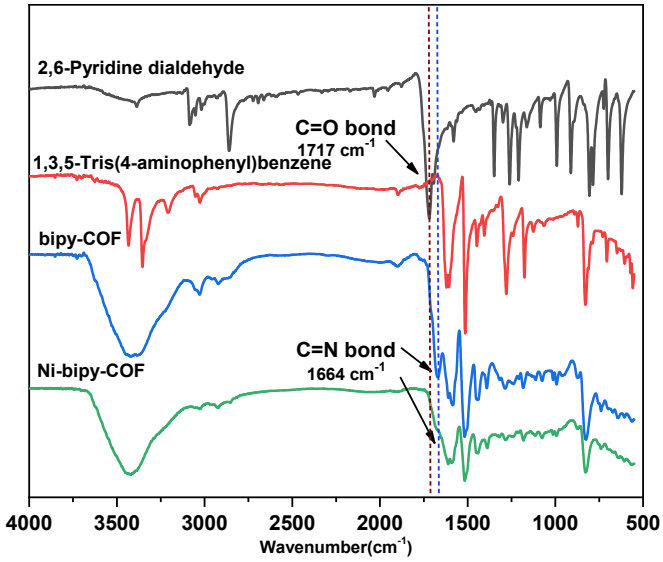

Figure S1. FT-IR spectra of bipy-COF (blue line), Ni-bipy-COF (green line), 2,6-pyridine dialdehyde (black line) and 1,3,5-tris(4-aminophenyl)benzene (red line).

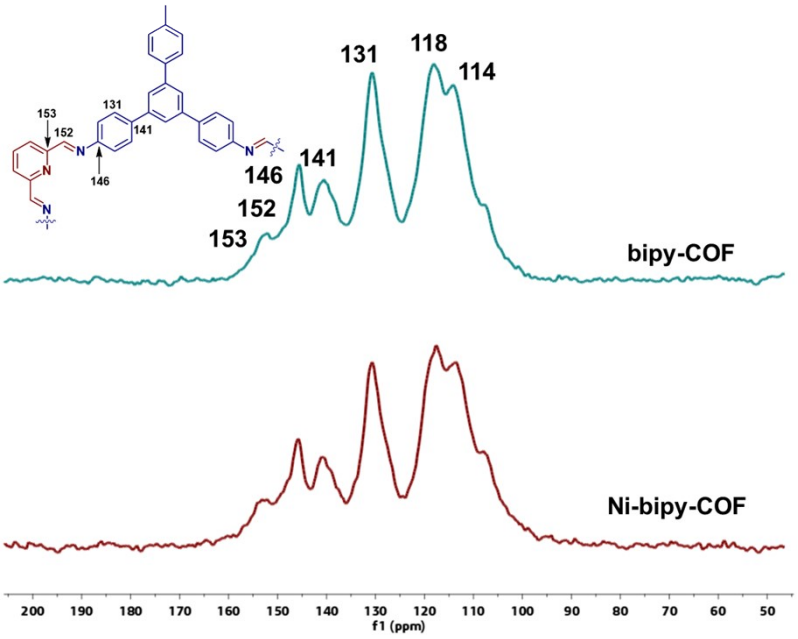

Figure S2. The ^{13}C CP/MAS NMR spectrum of bipy-COF and Ni-bipy-COF.

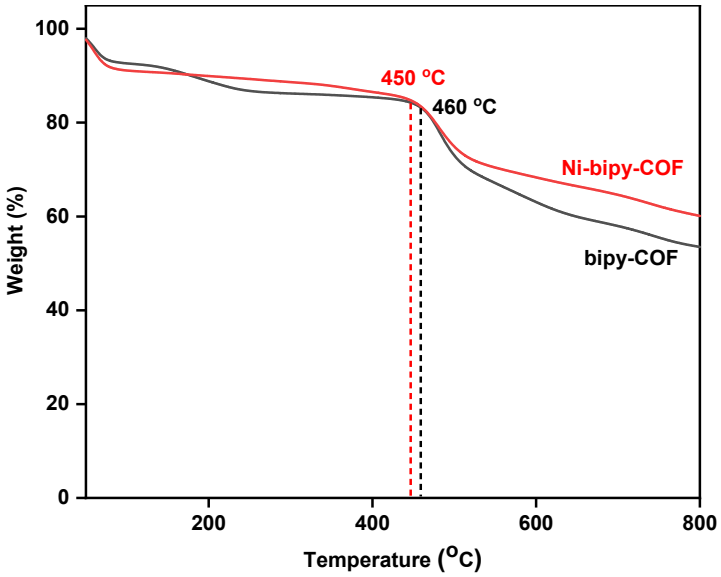

Figure S3. Thermogravimetric curves of bipy-COF (black) and Ni-bipy-COF (red).

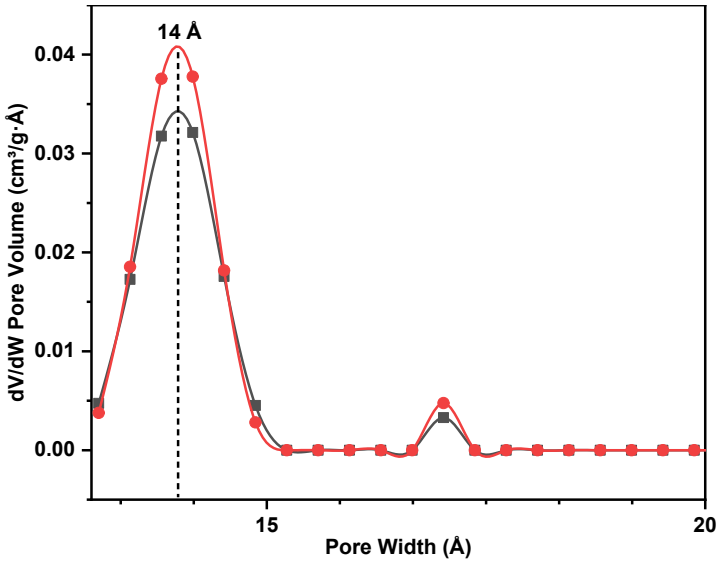

Figure S4. Pore size distributions of bipy-COF (red) and Ni-bipy-COF (black) calculated using non-local density functional theory.

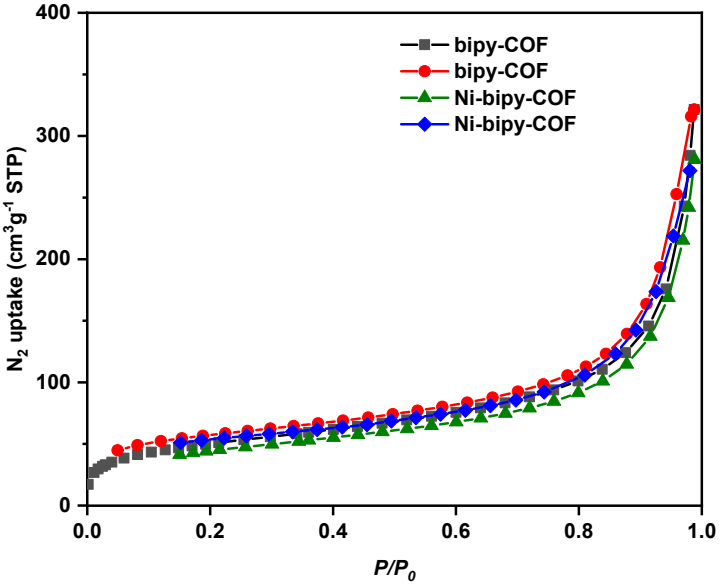

Figure S5. Nitrogen adsorption-desorption isotherms of bipy-COF and Ni-bipy-COF.

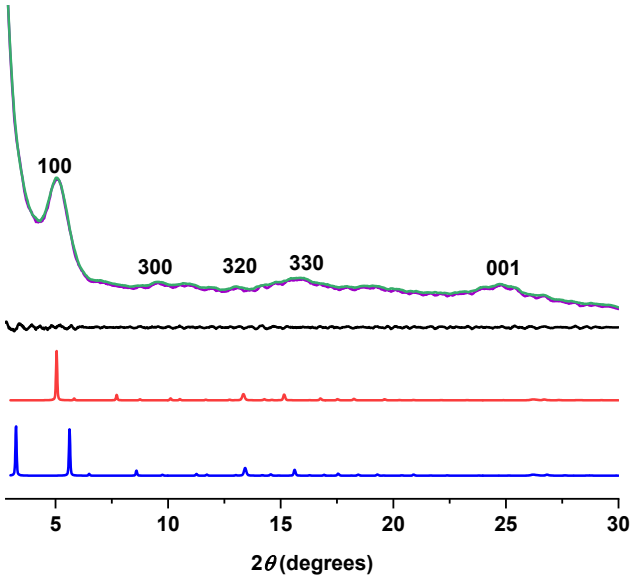

Figure S6. Experimental PXRD patterns of bipy-COF (purple), paw-ley-refined PXRD patterns of bipy-COF (green), and the corresponding difference (black); the calculated PXRD pat-terns for AA stacking (red) and AB stacking (blue).

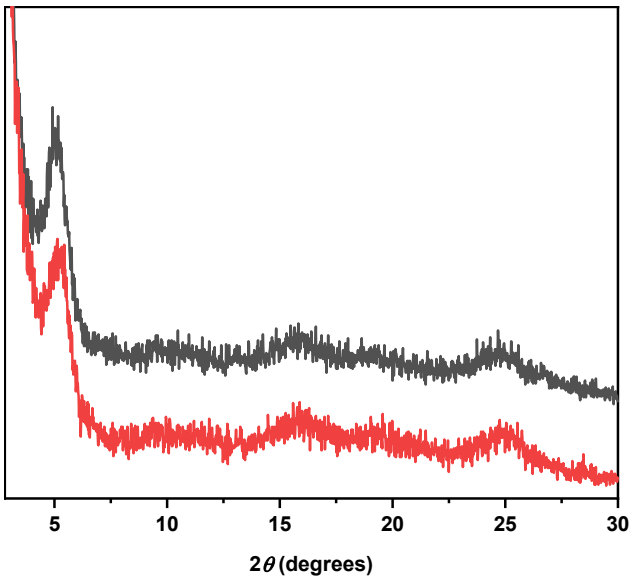

Figure S7. Chemical stability of bipy-COF after 24 h treatment under HCl (1 M, black) and NaOH (1M, black) at room temperature.

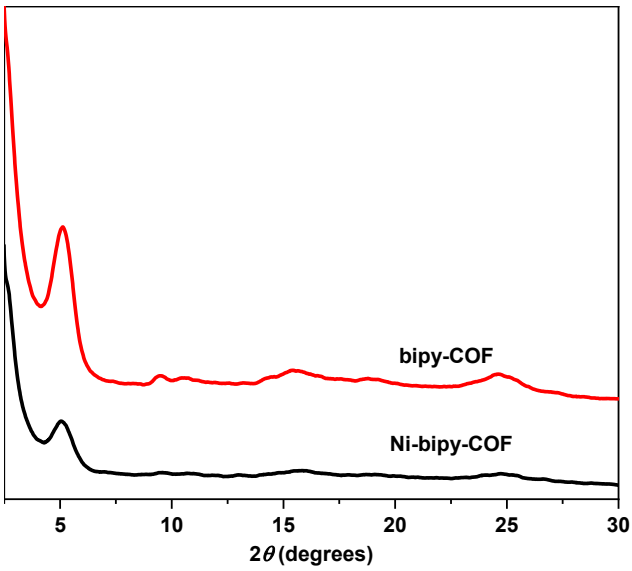

Figure S6. Experimental PXRD patterns of bipy-COF (red) and Ni-bipy-COF (black).

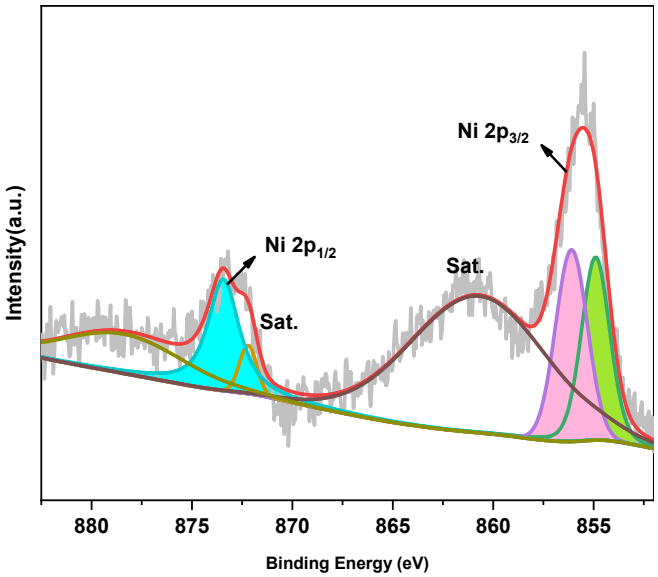

Figure S7. XPS Ni 2p spectra of Ni-bipy-COF.

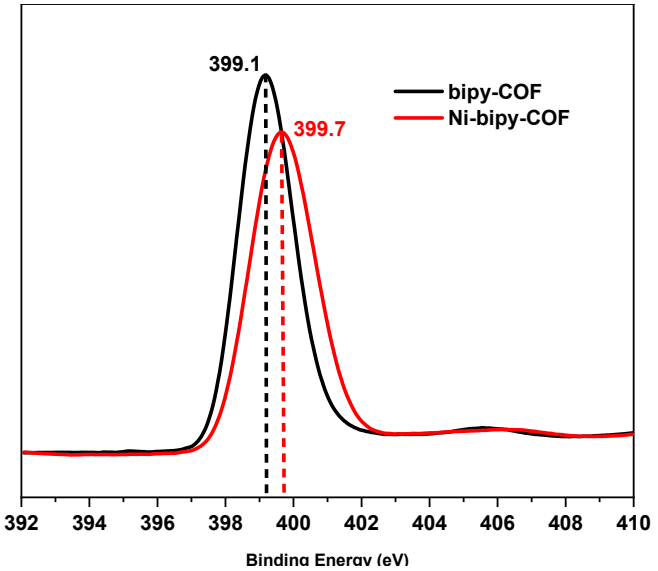

Figure S8. N 1s XPS spectra of bipy-COF (black) and Ni-bipy-COF (red).

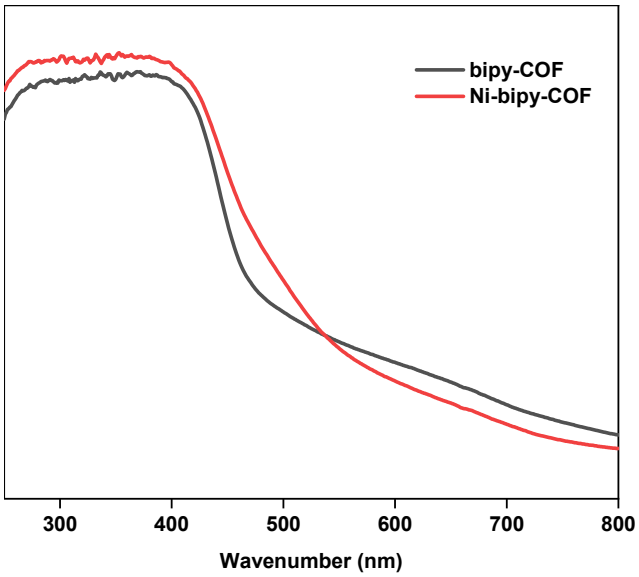

Figure S9. The solid-state UV-vis spectra of bipy-COF and Ni-bipy-COF

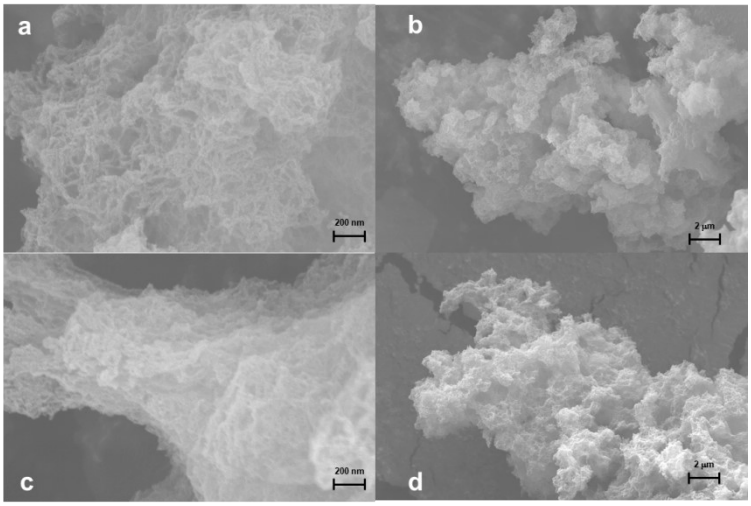

Figure S10. SEM images of bipy-COF (a, b) and Ni-bipy-COF (c, d).

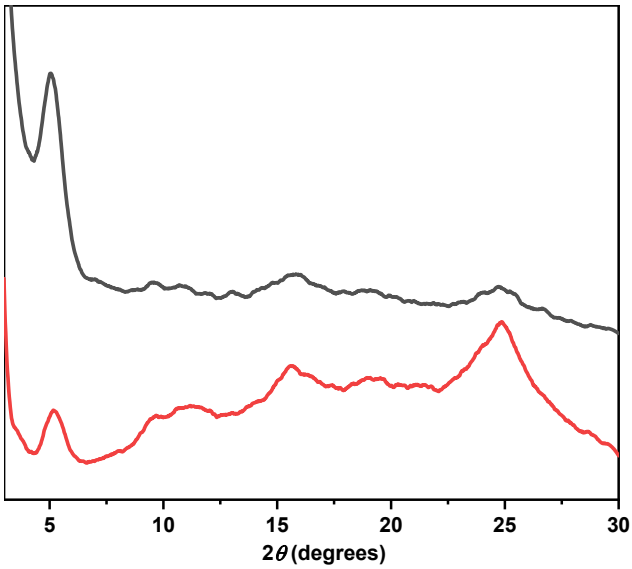

Figure S11. Experimental PXRD patterns of Ni-bipy-COF after the first cycle (black) and after the fifth cycle (red).

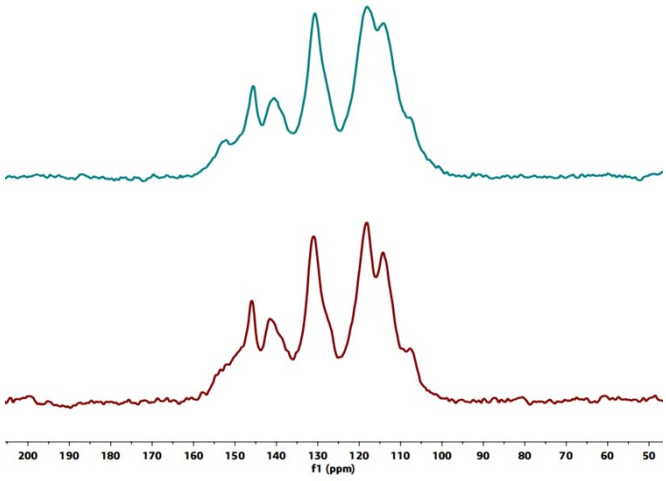

Figure S12. The ^{13}C CP/MAS NMR spectrum of Ni-bipy-COF before (green) and after the fifth cycle (red).

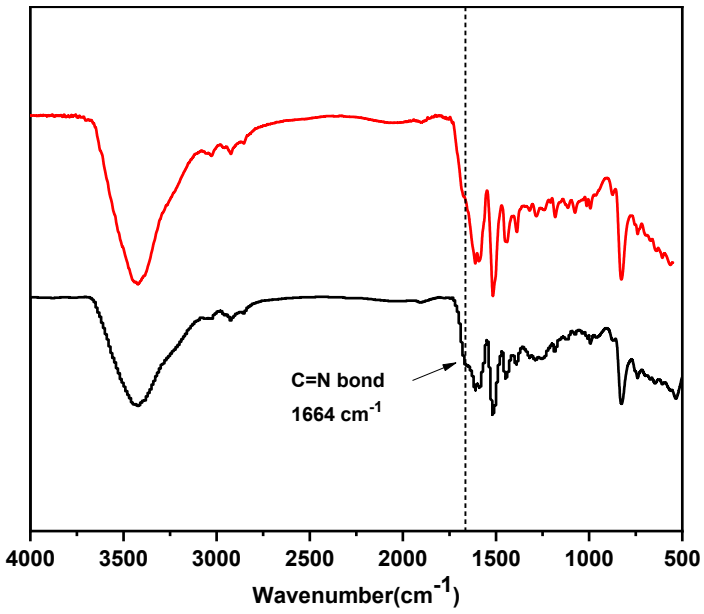

Figure S13. The FT-IR spectra of Ni-bipy-COF before (red) and after the fifth cycle (black) in the gram scale reaction.

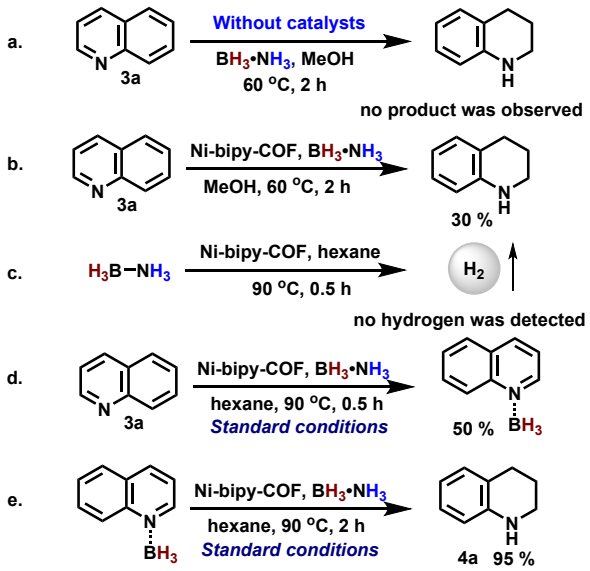

Figure S14. Control experiments.

To probe the mechanism of this reaction, control experiments were preformed (**Figure S14**). When the reaction was conducted without Ni-BIPY-COF catalyst, no product was observed (**Figure S14a**). When the reaction was conducted without quinolines as a hydrogen acceptor, no H_2 molecule was monitored (**Figure S14c**). These results demonstrated that this reaction is a catalytic transfer hydrogenation process. In addition, a key reaction intermediate, quinoline-borane (**Figure S14d**), was observed at the beginning of the reaction (**Scheme 3**), and this intermediate could be transformed into the target product **4a** with 95% yield under the standard conditions (**Figure S14e**), indicating quinoline-borane played a vital role in this catalytic transfer hydrogenation.

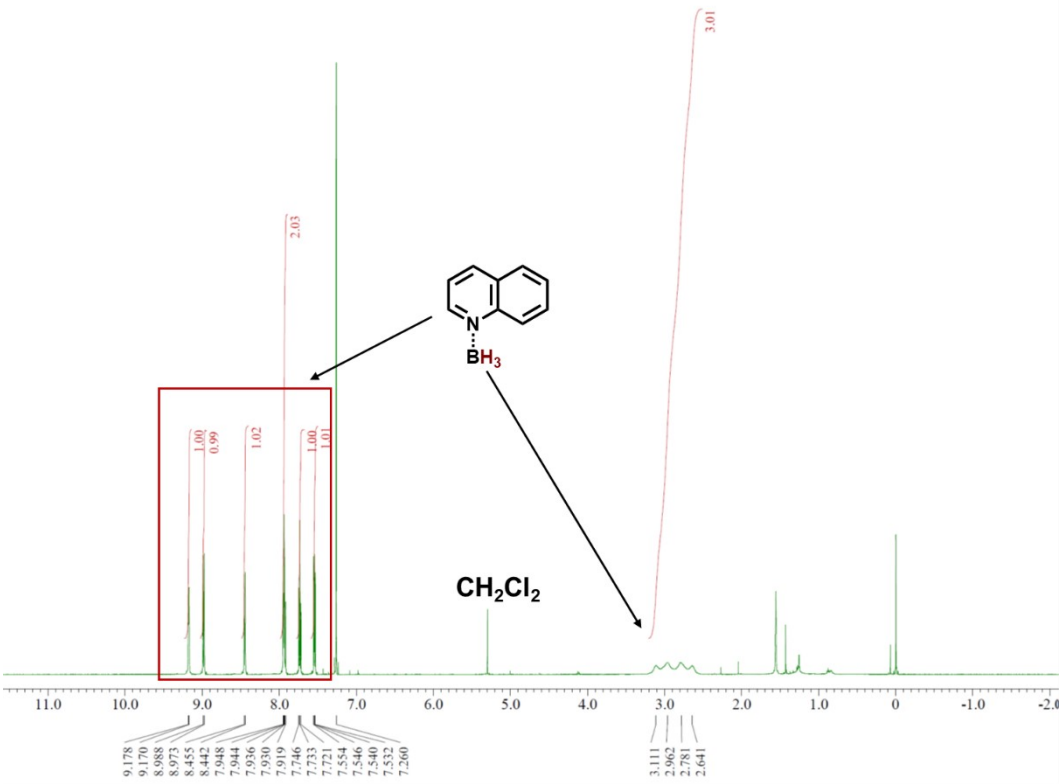

Figure S15. The experimental ^{1}H NMR spectra of quinoline-borane intermediate.

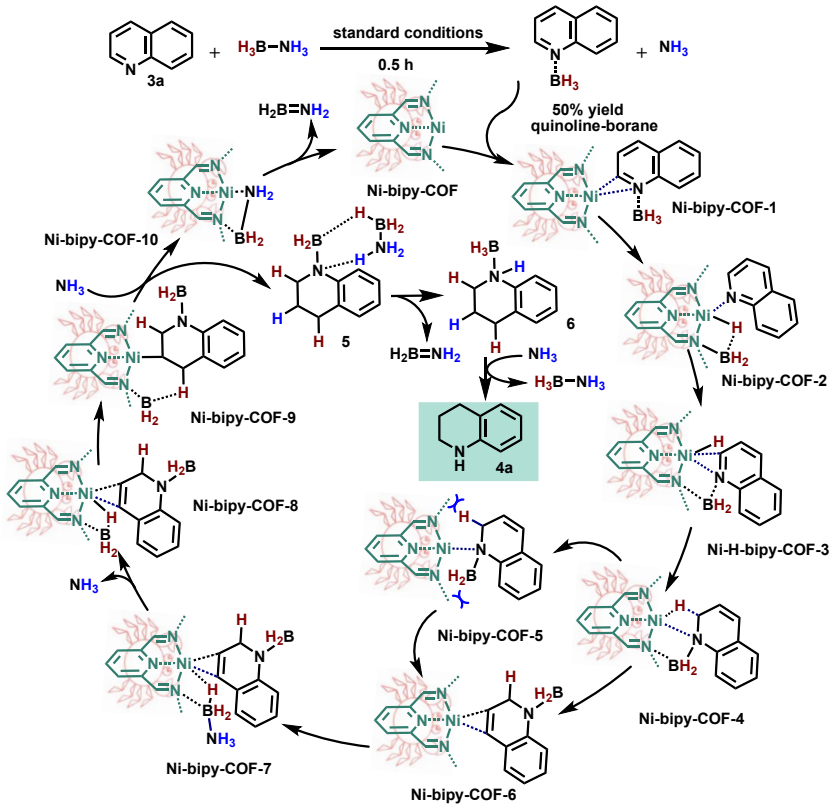

Figure S16. Plausible Mechanism.

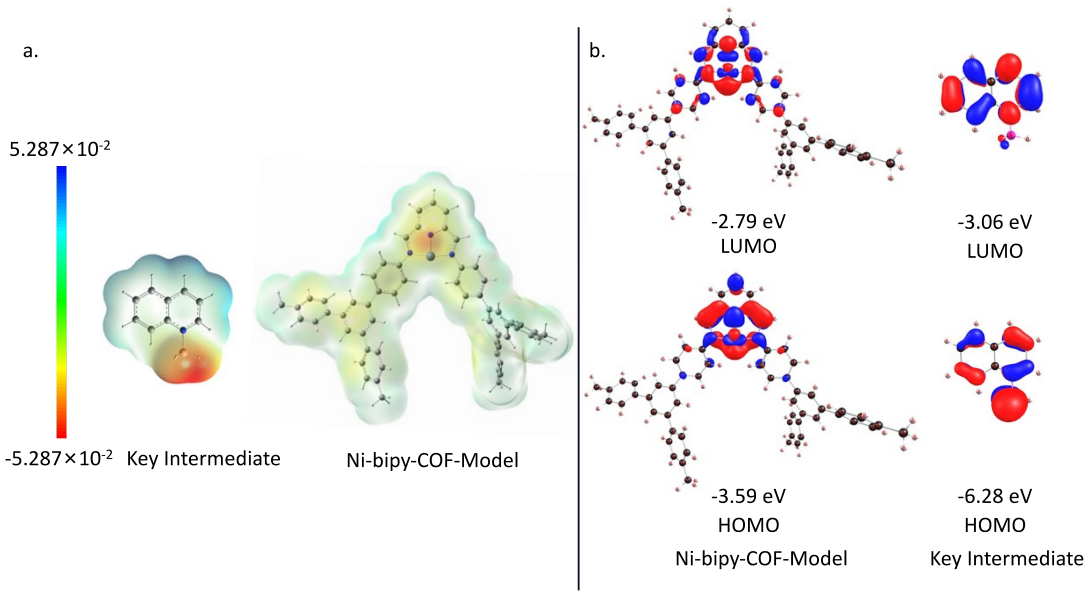

Figure S17 a. Optimized geometrical structures and the electronic potential surfaces for the key intermediate and the model systems of **Ni-bipy-COF**. The red, green, and blue regions indicate negative, neutral, and positive electrostatic potentials, respectively. **b**. Distributions of the highest occupied molecular orbital (HOMO) and the lowest unoccupied molecular orbital (LUMO) of the key intermediate and the model systems of **Ni-bipy-COF**, respectively. All calculations were performed at the theoretical level of M06L/6-311G(d) (SDD basis set for Ni).

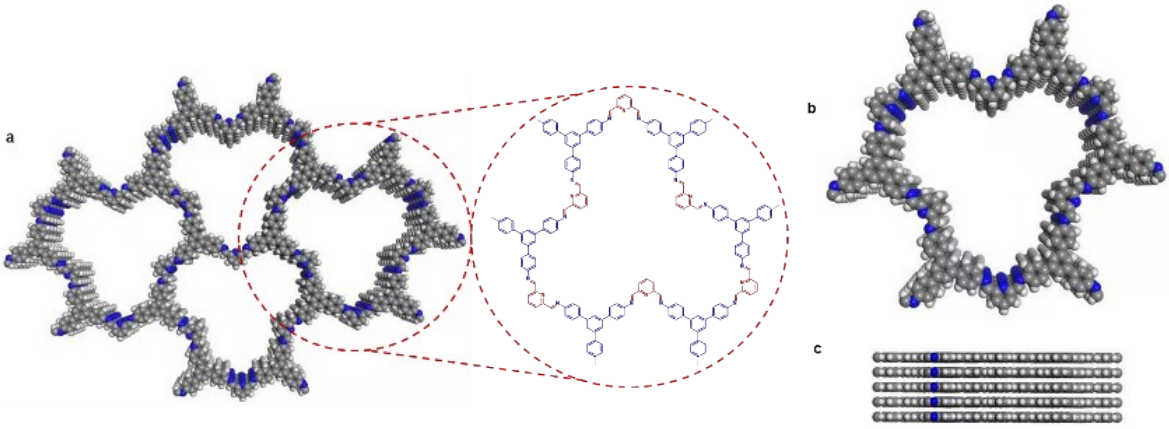

Figure S18. (a,b) Unit cell of eclipsed structure; (c) Side view of eclipsed structure. C: blue, N: red, and H: white.

Section D. Supporting Tables

Table S1. Optimization of reaction conditions for the Ni-bipy-COF-catalyzed transfer hydrogenation of **3a**. Conditions: **3a** (0.09747 mmol, 1.0 equiv), [Ni] (5 mg), AB (0.4873 mmol, 5.0 equiv), solvent (1.0 mL), 60~90 °C, 2 h.

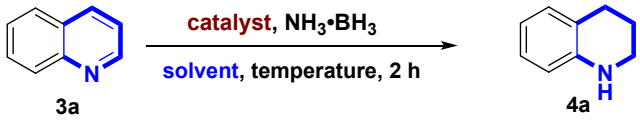

3a 4a

entry	solvent	catalyst	temperature	yield
1	MeOH	none	60 °C	none
2	MeOH	$Ni(OAc)_2$	60 °C	8 %
3	MeOH	Ni-bipy-COF	60 °C	30 %
4	MeOH	bipy-COF	60 °C	none
5	THF	Ni-bipy-COF	60 °C	53 %
6	hexane	Ni-bipy-COF	60 °C	81 %
7	Tol	Ni-bipy-COF	60 °C	23 %
8	H_2O	Ni-bipy-COF	60 °C	none
9	EtOH	Ni-bipy-COF	60 °C	20 %
10	H_2O	Ni-bipy-COF	90 °C	none
11	EtOH	Ni-bipy-COF	90 °C	28 %
12	hexane	Ni-bipy-COF	80 °C	90 %
13	hexane	Ni-bipy-COF	90 °C	98 %

Table S2. Optimization of the equivalents of $NH_3{\cdot}BH_3$. Reaction conditions: 0.09747 mmol of quinoline, 5.0 mg of Ni-bipy-COF, $NH_3{\cdot}BH_3$ (2.0-5.0 equiv), 1 mL of hexane, 90°C.

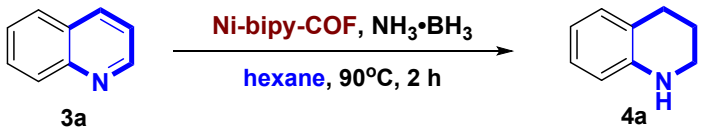

3a 4a

entry	the equivalents of $NH_3•BH_3$	yield
1	2	85%
2	3	90%
3	4	94%
4	5	98%

Table S3. Ni-bipy-COF-catalyzed transfer hydrogenation of quinolines. Reaction conditions: 1 mmol of quinolines, 50.0 mg of Ni-bipy-COF, $NH_3{\cdot}BH_3$ (5.0 equiv), 10 mL of hexane, 90℃.

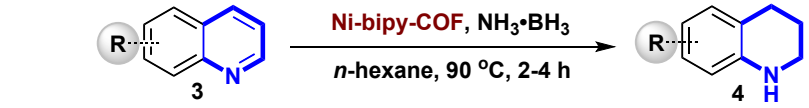

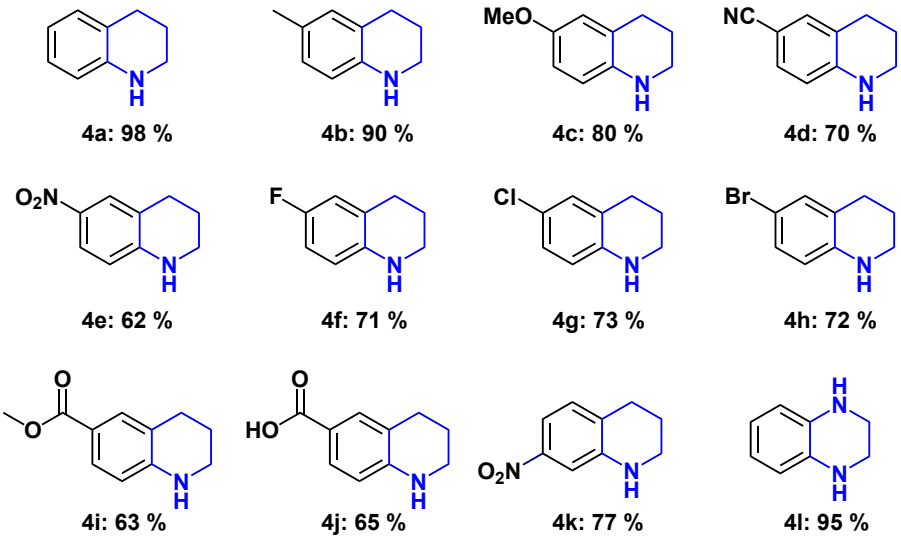

Table S4. The yields of 1, 2, 3, 4-tetrahydroquinoline catalyzed by Ni-bipy-COF for 5 reaction cycles. Reaction conditions: 1 mmol of quinoline, 50.0 mg of Ni-bipy-COF, $NH_3{\cdot}BH_3$ (5.0 equiv), 10 mL of hexane, 90℃.

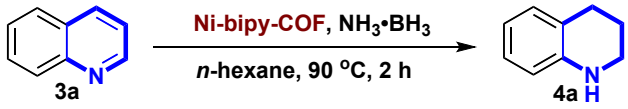

cycle	1	2	3	4	5
yield	95	93	94	92	90

Table S5. The gram scale reaction and yields of 1, 2, 3, 4-tetrahydroquinoline for 5 reaction cycles. Reaction conditions: 1.0 g of quinolines (7.7 mmol), 387 mg of Ni-bipy-COF, $NH_3{\cdot}BH_3$ (5.0 equiv), 77 mL of hexane, 90℃, in a 350 mL sealed glass tube.

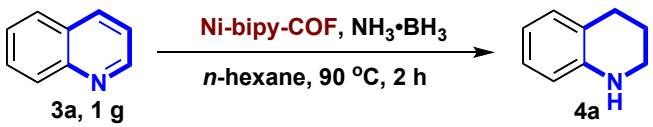

cycle	1	2	3	4	5
yield	96	95	93	94	91

Table S6. Elemental analysis of bipy-COF.

		C (%)	H (%)	N (%)
bipy-COF	Calcd.	83.01	4.49	12.49
	Found	82.96	4.59	12.35

Table S7. Atomistic coordinates for the AA-stacking mode of Ni-bipy-COF optimized using DFTB+ method. Space group: P6; α = β = 90°, γ = 120°, a = 35.1635 Å, b = 35.1635 Å, c = 3.445827 Å.

C1	C	0.34446	0.71557	1/2	1	0
C2	C	0.33735	0.67181	1/2	1	0
C3	C	0.37288	0.66324	1/2	1	0
C4	C	0.41697	0.69769	1/2	1	0
C5	C	0.42395	0.74110	1/2	1	0
C6	C	0.38909	0.74958	1/2	1	0
N7	N	0.45326	0.68805	1/2	1	0
C8	C	0.49478	0.71902	1/2	1	0
C9	C	0.30686	0.72636	1/2	1	0
C10	C	0.26171	0.69301	1/2	1	0
C11	C	0.22684	0.70283	1/2	1	0
C12	C	0.23900	0.74792	1/2	1	0
C13	C	0.28318	0.78273	1/2	1	0
C14	C	0.31613	0.77077	1/2	1	0
C15	C	0.29476	0.83129	1/2	1	0
C16	C	0.17793	2/3	1/2	1	0
C17	C	0.26154	0.84317	1/2	1	0
C18	C	0.27159	0.88717	1/2	1	0
C19	C	0.31559	0.92214	1/2	1	0
C20	C	0.34895	0.91123	1/2	1	0
C21	C	0.33900	0.86700	1/2	1	0
C22	C	0.16464	0.62133	1/2	1	0
C23	C	0.11995	0.58837	1/2	1	0
C24	C	0.08606	0.59915	1/2	1	0
C25	C	0.09859	0.64373	1/2	1	0
C26	C	0.14317	0.67677	1/2	1	0
N27	N	0.32756	0.96838	1/2	1	0
C28	C	0.29941	0.98249	1/2	1	0
N29	N	0.03924	0.56653	1/2	1	0
C30	C	0.02298	0.52397	1/2	1	0
C31	C	0.53503	0.71437	1/2	1	0

N32	N	0.53610	0.67538	1/2	1	0
C33	C	0.57619	0.67645	1/2	1	0
C34	C	0.61570	0.71731	1/2	1	0
C35	C	0.61492	0.75624	1/2	1	0
C36	C	0.57496	0.75495	1/2	1	0
C37	C	0.58283	0.63749	1/2	1	0
N38	N	0.55254	0.59590	1/2	1	0
C39	C	0.56257	0.56003	1/2	1	0
C40	C	0.60603	0.56695	1/2	1	0
C41	C	0.61427	0.53174	1/2	1	0
C42	C	0.57984	0.48734	1/2	1	0
C43	C	0.53622	0.48074	1/2	1	0
C44	C	0.52803	0.51628	1/2	1	0
C45	C	0.58955	0.44906	1/2	1	0
C46	C	0.63336	0.45632	1/2	1	0
C47	C	0.64285	0.42143	1/2	1	0
C48	C	0.60625	0.37791	1/2	1	0
C49	C	0.56200	0.36831	1/2	1	0
C50	C	0.55488	0.40471	1/2	1	0
C51	C	0.69044	0.42989	1/2	1	0
C52	C	0.69909	0.39440	1/2	1	0
C53	C	0.74191	0.40133	1/2	1	0
C54	C	0.77856	0.44359	1/2	1	0
C55	C	0.77172	0.47979	1/2	1	0
C56	C	0.72833	0.47306	1/2	1	0
C57	C	0.52349	0.32055	1/2	1	0
C58	C	0.52988	0.28336	1/2	1	0
C59	C	0.49417	0.23978	1/2	1	0
C60	C	0.45076	0.23171	1/2	1	0
C61	C	0.44382	0.26760	1/2	1	0
C62	C	0.47904	0.31092	1/2	1	0
N63	N	0.41231	0.18834	1/2	1	0
N64	N	0.82112	0.44651	1/2	1	0
C65	C	0.86156	0.47952	1/2	1	0
C66	C	0.89817	0.46913	1/2	1	0
C67	C	0.40830	0.14924	1/2	1	0
C68	C	0.36306	0.10984	1/2	1	0
C69	C	0.32650	0.11644	1/2	1	0
C70	C	0.28372	0.08096	1/2	1	0
C71	C	0.27632	0.03815	1/2	1	0
C72	C	0.31161	0.02976	1/2	1	0
C73	C	0.35542	0.06596	1/2	1	0
C74	C	0.88716	0.42449	1/2	1	0

C75	C	0.92004	0.41345	1/2	1	0
C76	C	0.96388	0.44645	1/2	1	0
C77	C	0.97502	0.49092	1/2	1	0
N78	N	0.94202	0.50147	1/2	1	0
H79	H	0.30463	0.64346	1/2	1	0
H80	H	0.36584	0.62940	1/2	1	0
H81	H	0.45609	0.77013	1/2	1	0
H82	H	0.39921	0.78401	1/2	1	0
H83	H	0.50288	0.75285	1/2	1	0
H84	H	0.25390	0.65936	1/2	1	0
H85	H	0.21368	0.75603	1/2	1	0
H86	H	0.34931	0.79673	1/2	1	0
H87	H	0.22690	0.81941	1/2	1	0
H88	H	0.24388	0.89258	1/2	1	0
H89	H	0.38314	0.93730	1/2	1	0
H90	H	0.36705	0.86221	1/2	1	0
H91	H	0.18806	0.60994	1/2	1	0
H92	H	0.11298	0.55470	1/2	1	0
H93	H	0.07344	0.65314	1/2	1	0
H94	H	0.14872	0.70984	1/2	1	0
H95	H	0.26451	0.95934	1/2	1	0
H96	H	0.04478	0.51055	1/2	1	0
H97	H	0.64764	0.71935	1/2	1	0
H98	H	0.64544	0.78756	1/2	1	0
H99	H	0.57551	0.78619	1/2	1	0
H100	H	0.61695	0.64631	1/2	1	0
H101	H	0.63493	0.59924	1/2	1	0
H102	H	0.64851	0.54090	1/2	1	0
H103	H	0.50731	0.44849	1/2	1	0
H104	H	0.49426	0.50950	1/2	1	0
H105	H	0.66044	0.48922	1/2	1	0
H106	H	0.61197	0.35093	1/2	1	0
H107	H	0.52199	0.39860	1/2	1	0
H108	H	0.67375	0.36032	1/2	1	0
H109	H	0.74662	0.37299	1/2	1	0
H110	H	0.79952	0.51307	1/2	1	0
H111	H	0.72559	0.50235	1/2	1	0
H112	H	0.56203	0.28648	1/2	1	0
H113	H	0.50080	0.21274	1/2	1	0
H114	H	0.41042	0.26191	1/2	1	0
H115	H	0.46977	0.33591	1/2	1	0
H116	H	0.86849	0.51330	1/2	1	0
H117	H	0.43696	0.14516	1/2	1	0

H118	H	0.33075	0.14928	1/2	1	0
H119	H	0.25606	0.08669	1/2	1	0
H120	H	0.24248	0.01126	1/2	1	0
H121	H	0.38304	0.06016	1/2	1	0
H122	H	0.85321	0.39792	1/2	1	0
H123	H	0.91150	0.37916	1/2	1	0
H124	H	0.98912	0.43716	1/2	1	0

Section E. ^{1}H NMR and ^{13}C NMR Spectra of THQs

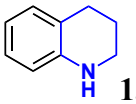

1,2,3,4-tetrahydroquinoline (4a): Yellow oil; 98% yield; ^{1}H NMR (400 MHz, $CDCl_3$) δ 6.98 ((ddd, *J* = 14.5, 7.5, 1.5 Hz, 2H), 6.63 ((td, *J* = 7.4, 1.2 Hz, 1H), 6.49 (dd, *J* = 7.9, 1.2 Hz, 1H), 3.91 (ms, 1H), 3.33-3.30 (m, 2H), 2.78 (t, *J* = 6.4 Hz, 2H), 1.99-1.93 (m, 2H); ^{13}C NMR (100 MHz, $CDCl_3$) δ 144.82, 129.55, 126.76, 121.48, 116.97, 114.22, 42.02, 27.01, 22.22.

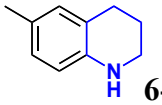

6-methyl-1,2,3,4-tetrahydroquinoline (4b): Yellow solid; 90% yield; ^{1}H NMR (400 MHz, $CDCl_3$) δ 6.79 (d, *J* = 5.6 Hz, 2H), 6.47-6.38 (m, 1H), 3.34-3.21 (m, 2H), 2.74 (t, *J* = 6.4 Hz, 2H), 2.21 (s, 3H), 2.00-1.86 (m, 2H); ^{13}C NMR (100 MHz, $CDCl_3$) δ 142.48, 130.14, 127.31, 126.33, 121.68, 114.53, 42.25, 26.97, 22.50, 20.47.

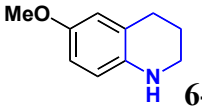

6-methoxy-1,2,3,4-tetrahydroquinoline (4c): Yellow solid; 80% yield; ^{1}H NMR (400 MHz, $CDCl_3$) δ 6.59 (dt, *J* = 8.8, 2.8 Hz, 2H), 6.46 (d, *J* = 8.5 Hz, 1H), 3.74 (s, 3H), 3.33-3.20 (m, 2H), 2.76 (t, *J* = 6.5 Hz, 2H), 2.02-1.89 (m, 2H); ^{13}C NMR (100 MHz, $CDCl_3$) δ 151.86, 138.92, 122.92, 115.61, 114.92, 112.94, 55.85, 42.38, 27.21, 22.48.

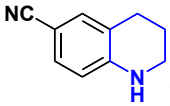

1,2,3,4-tetrahydroquinoline-6-carbonitrile (4d): Yellow oil; 70% yield; ^{1}H NMR (400 MHz, $CDCl_3$) δ 7.23-7.14 (m, 2H), 6.38 (d, *J* = 8.2 Hz, 1H), 4.38 (s, 1H), 3.55-3.21 (m, 2H), 2.73 (t, *J* = 6.3 Hz, 2H), 2.12-1.72 (m, 2H); ^{13}C NMR (100 MHz, $CDCl_3$) δ 148.27, 133.28, 131.33, 120.99, 120.89, 113.29, 97.78, 41.63, 26.77, 21.01.

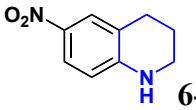

6-nitro-1,2,3,4-tetrahydroquinoline (4e): Brown solid; 62% yield; ^{1}H NMR (400 MHz, $CDCl_3$) δ 8.12-7.69 (m, 2H), 6.53-6.15 (m, 1H), 4.78 (ms, 1H), 3.41 (td, *J* = 5.9, 2.6 Hz, 2H), 2.78 (t, *J* = 6.3 Hz, 2H), 1.94 (dt, *J* = 12.2, 6.1 Hz, 2H); ^{13}C NMR (100 MHz, $CDCl_3$) δ 150.49, 137.21, 125.96, 124.34, 119.88, 112.20, 41.78, 26.93, 20.85.

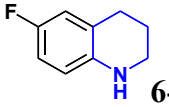

6-fluoro-1,2,3,4-tetrahydroquinoline (4f): Yellow oil; 71% yield; ^{1}H NMR (400 MHz, $CDCl_3$) δ 6.79-6.60 (m, 2H), 6.40 (dd, *J* = 9.4, 4.9 Hz, 1H), 3.56 (s,

1H), 3.33-3.19 (m, 2H), 2.75 (t, J = 6.5 Hz, 2H), 2.03-1.83 (m, 2H); ^{13}C NMR (100 MHz, $CDCl_3$) δ 155.46 (d, J = 233.0 Hz), 140.98 (d, J = 2.0 Hz), 122.80 (d, J = 7.0 Hz), 115.63 (d, J = 21.0 Hz), 114.93 (d, J = 8.0 Hz), 113.20 (d, J = 22.0 Hz), 42.10, 27.05 (d, J = 2.0 Hz), 22.01.

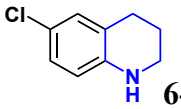

6-chloro-1,2,3,4-tetrahydroquinoline (4g): Yellow solid; 73% yield; ^{1}H NMR (400 MHz, $CDCl_3$) δ 7.05-6.65 (m, 2H), 6.39 (t, J = 5.1 Hz, 1H), 3.58 (s, 1H), 3.28 (dd, J = 6.9, 4.1 Hz, 2H), 2.73 (t, J = 6.4 Hz, 2H), 1.92 (ddd, J = 11.7, 8.7, 6.4 Hz, 2H); ^{13}C NMR (100 MHz, $CDCl_3$) δ 143.34, 129.05, 126.53, 122.90, 121.15, 115.12, 41.88, 26.90, 21.77.

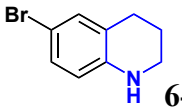

6-bromo-1,2,3,4-tetrahydroquinoline (4h): Yellow oil; 72% yield; ^{1}H NMR (400 MHz, $CDCl_3$) δ 7.03 (dt, J = 8.3, 2.2 Hz, 2H), 6.33 (d, J = 8.3 Hz, 1H), 3.83 (ms, 1H), 3.46-3.17 (m, 2H), 2.72 (t, J = 6.4 Hz, 2H), 2.07-1.80 (m, 2H); ^{13}C NMR (100 MHz, $CDCl_3$) δ 143.79, 131.92, 129.42, 123.44, 115.57, 108.25, 41.85, 26.89, 21.74.

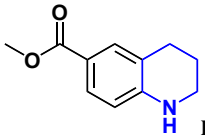

methyl-1,2,3,4-tetrahydroquinoline-6-carboxylate (4i): White solid; 63% yield; ^{1}H NMR (400 MHz, $CDCl_3$) δ 7.73-7.55 (m, 2H), 6.45-6.32 (m, 1H), 4.35 (ms, 1H), 3.83 (s, 3H), 3.47-3.25 (m, 2H), 2.76 (t, J = 6.3 Hz, 2H), 2.04-1.83 (m, 2H); ^{13}C NMR (100 MHz, $CDCl_3$) δ 167.59, 148.84, 131.34, 129.15, 119.93, 117.42, 112.66, 51.48, 41.74, 26.94, 21.44.

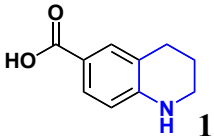

1,2,3,4-tetrahydroquinoline-6-carboxylic acid (4j): Yellow solid; 65% yield; ^{1}H NMR (400 MHz, $CDCl_3$) δ 7.80-7.64 (m, 2H), 6.47-6.31 (m, 1H), 3.49-3.19 (m, 2H), 2.78 (t, J = 6.3 Hz, 2H), 1.93 (td, J = 11.4, 6.2 Hz, 2H); ^{13}C NMR (100 MHz, $CDCl_3$) δ 172.63, 149.54, 132.08, 130.02, 119.97, 116.48, 112.69, 41.80, 26.94, 21.39.

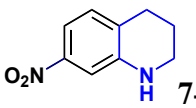

7-nitro-1,2,3,4-tetrahydroquinoline (4k): Yellow solid; 77% yield; ^{1}H NMR (400 MHz, $CDCl_3$) δ 7.39 (dd, J = 8.2, 2.3 Hz, 1H), 7.28-7.25 (m, 1H), 7.01 (d, J = 8.2 Hz, 1H), 4.19 (ms, 1H), 3.49-3.19 (m, 2H), 2.81 (t, J = 6.4 Hz, 2H), 2.12-1.83

(m, 2H); ^{13}C NMR (100 MHz, $CDCl_3$) δ 147.30, 145.21, 129.76, 128.35, 111.32, 107.84, 41.59, 27.31, 21.14.

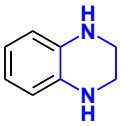

1,2,3,4-tetrahydroquinoxaline (4l): Yellow brown solid; 95% yield; ^{1}H NMR (400 MHz, $CDCl_3$) δ 6.61-6.57 (m, 2H), 6.52-6.48 (m, 2H), 3.42 (s, 4H); ^{13}C NMR (100 MHz, $CDCl_3$) δ 133.74, 118.83, 114.78, 41.45.

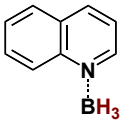

quinoline-borane intermediate: Wite solid; 50% yield; ^{1}H NMR (400 MHz, $CDCl_3$) δ 9.17 (d, J = 3.2 Hz, 1H), 8.98 (d, J = 6.0 Hz, 1H), 8.45 (d, J = 5.2 Hz, 1H), 7.95-7.92 (m, 2H), 7.73 (t, J = 6.4 Hz, 1H), 7.54 (dd, J = 3.2, 5.6 Hz, 1H), 3.11-2.64 (m, 3H).

Section F. Copies of NMR Spectra

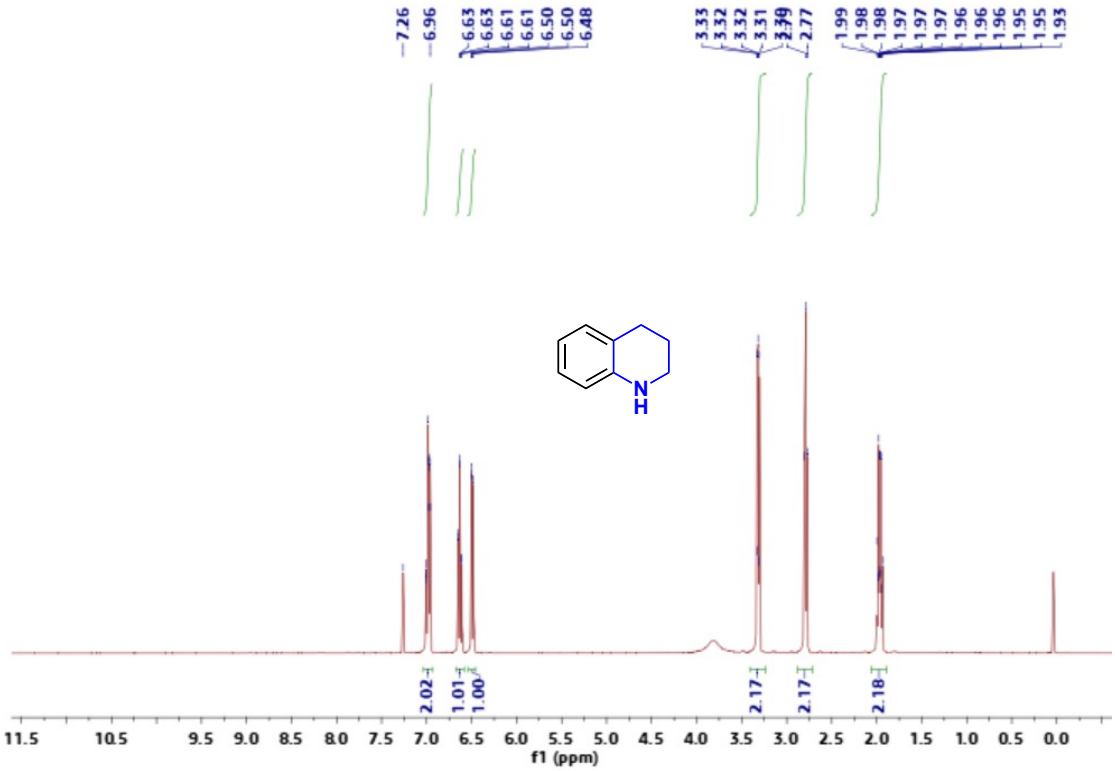

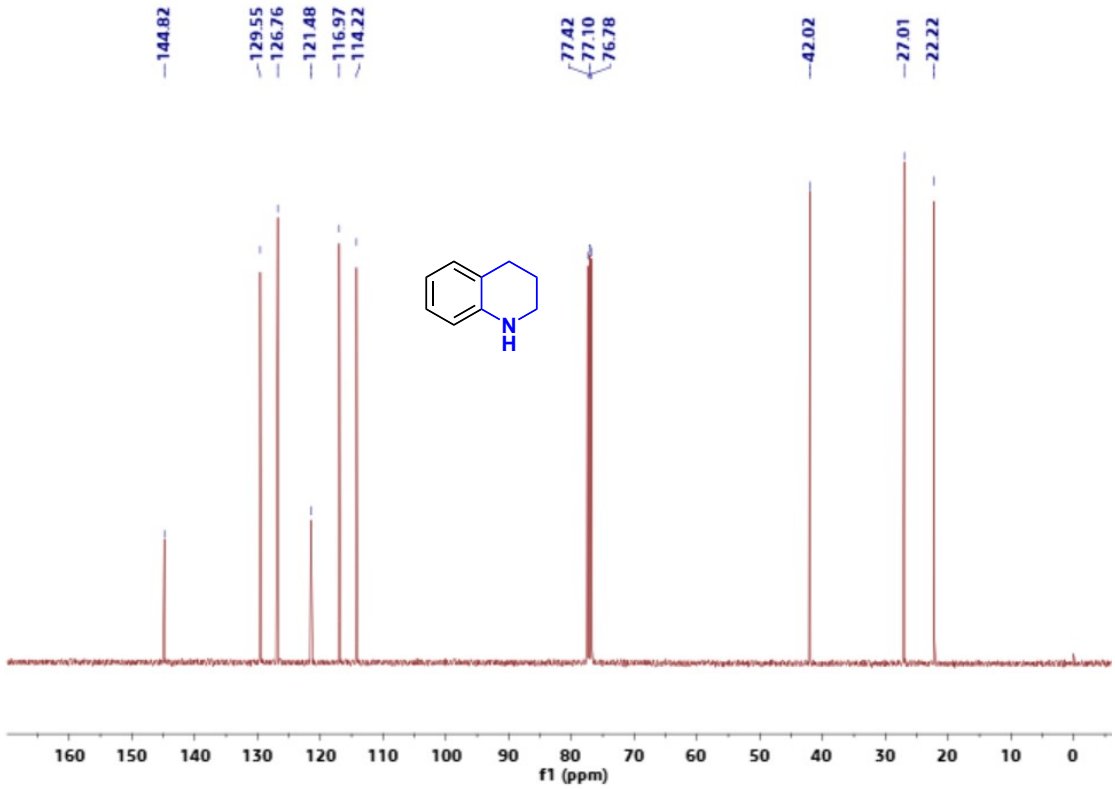

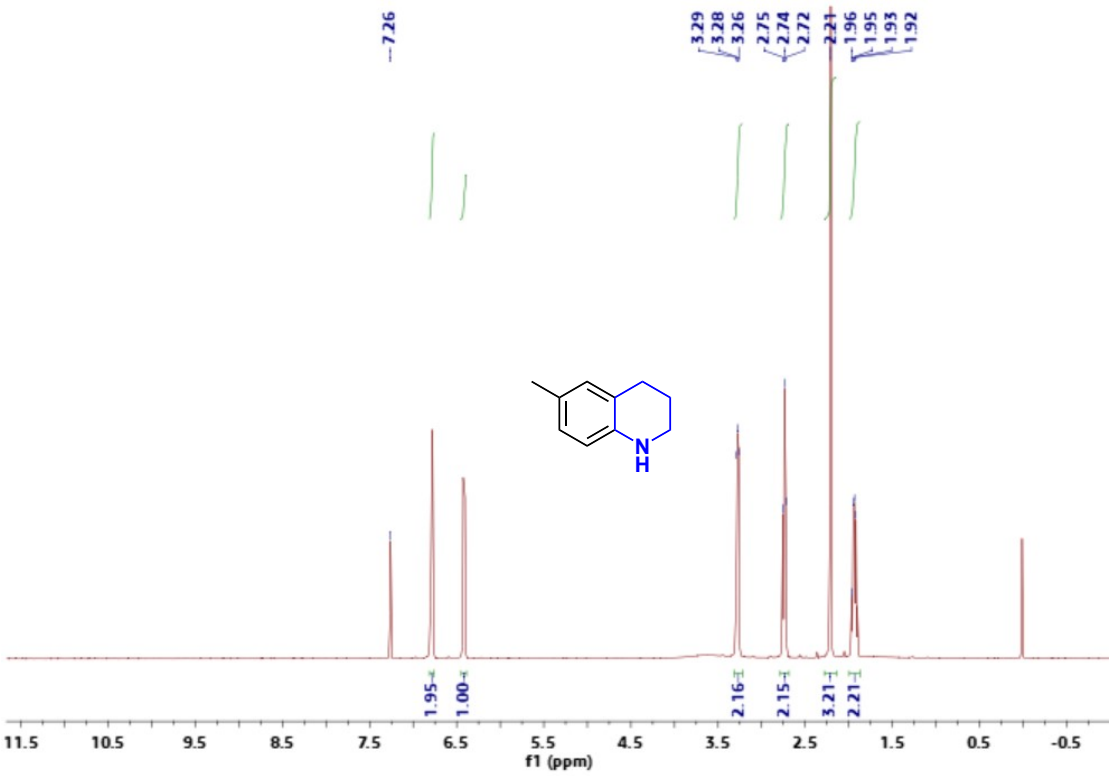
7.26
3.29
3.28
3.26
2.75
2.74
2.72
2.21
1.96
1.95
1.93
1.92
1.95
1.00
2.16
2.15
3.21
2.21
11.5
10.5
9.5
8.5
7.5
6.5
5.5
4.5
3.5
2.5
1.5
0.5
-0.5
f1 (ppm)

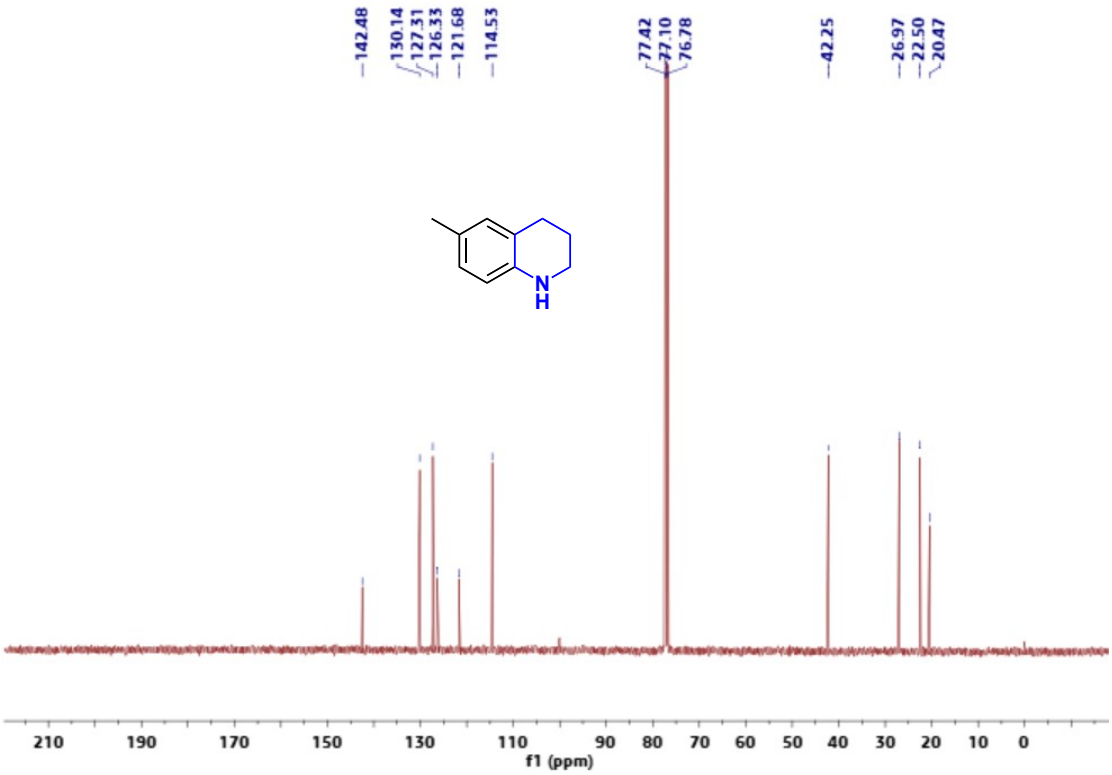
142.48
130.14
127.31
126.33
121.68
114.53
77.42
77.10
76.78
42.25
26.97
22.50
20.47
210
190
170
150
130
110
90
80
70
60
50
40
30
20
10
0
f1 (ppm)

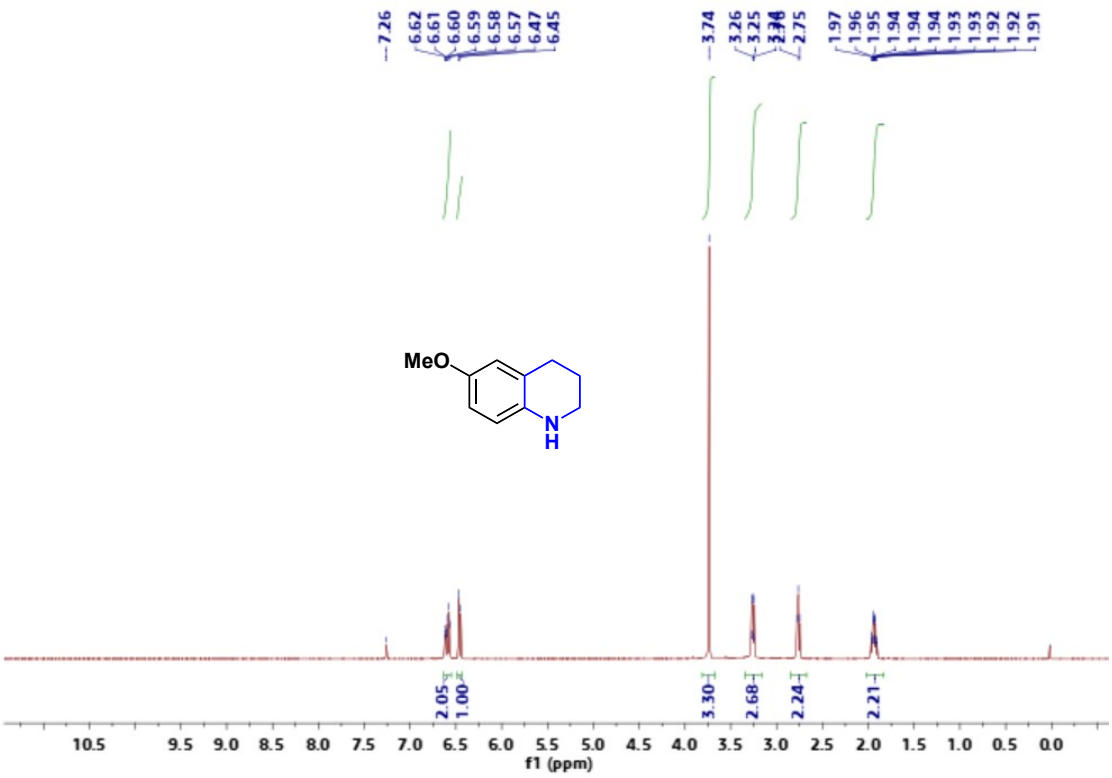
7.26
6.62
6.61
6.60
6.59
6.58
6.57
6.47
6.45
3.74
3.26
3.25
2.75
1.97
1.96
1.95
1.94
1.94
1.94
1.93
1.92
1.92
1.91
MeO
N
H
2.05
1.00
3.30
2.68
2.24
2.21
10.5
9.5
9.0
8.5
8.0
7.5
7.0
6.5
6.0
5.5
5.0
4.5
4.0
3.5
3.0
2.5
2.0
1.5
1.0
0.5
0.0
f1 (ppm)

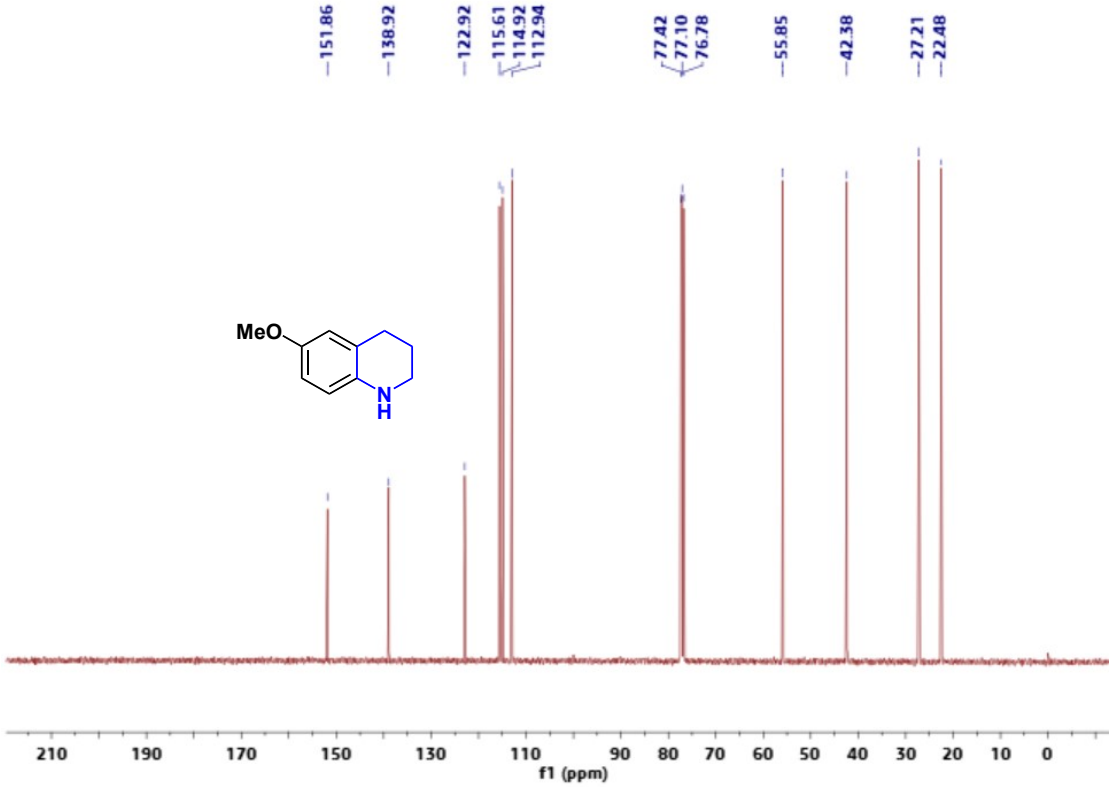
151.86
138.92
122.92
115.61
114.92
112.94
77.42
77.10
76.78
55.85
42.38
27.21
22.48
MeO
N
H
210
190
170
150
130
110
90
80
70
60
50
40
30
20
10
0
f1 (ppm)

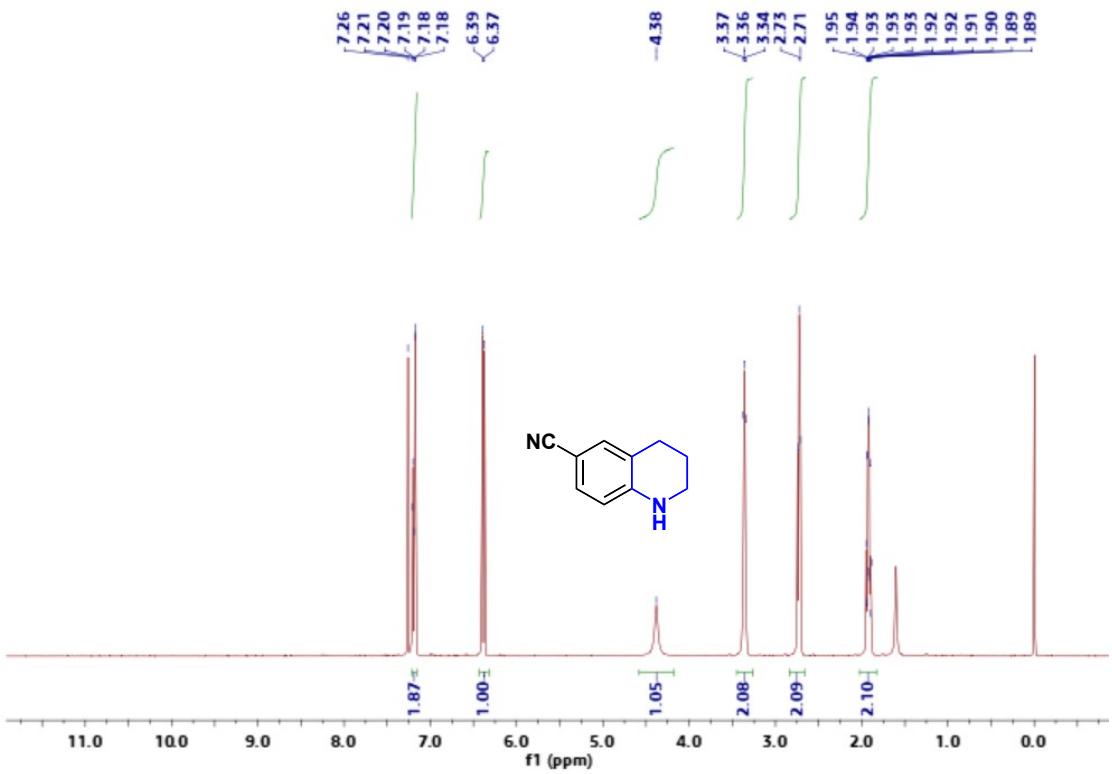
7.26
7.21
7.20
7.19
7.18
7.18
6.39
6.37
4.38
3.37
3.36
3.34
2.73
2.71
1.95
1.94
1.93
1.93
1.93
1.92
1.92
1.91
1.90
1.89
1.89
NC
N
H
1.87
1.00
1.05
2.08
2.09
2.10
11.0
10.0
9.0
8.0
7.0
6.0
5.0
4.0
3.0
2.0
1.0
0.0
f1 (ppm)

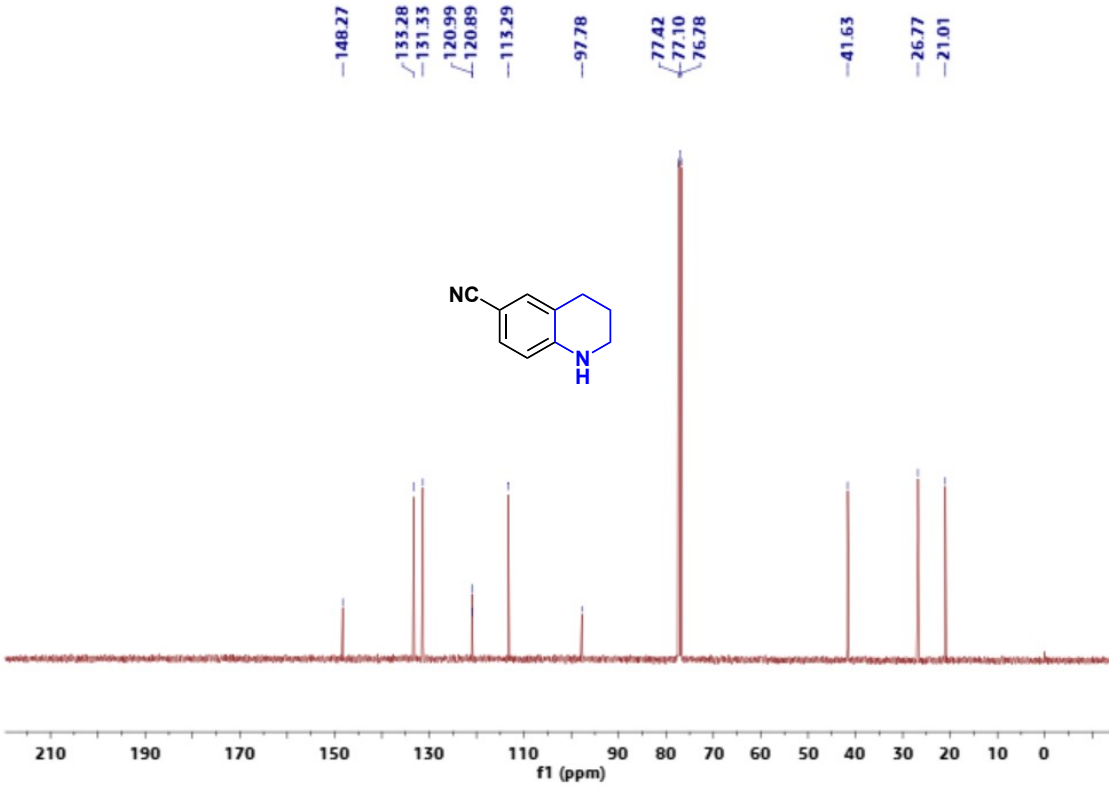
148.27
133.28
131.33
120.99
120.89
113.29
97.78
77.42
77.10
76.78
41.63
26.77
21.01
NC
N
H
210
190
170
150
130
110
90
80
70
60
50
40
30
20
10
0
f1 (ppm)

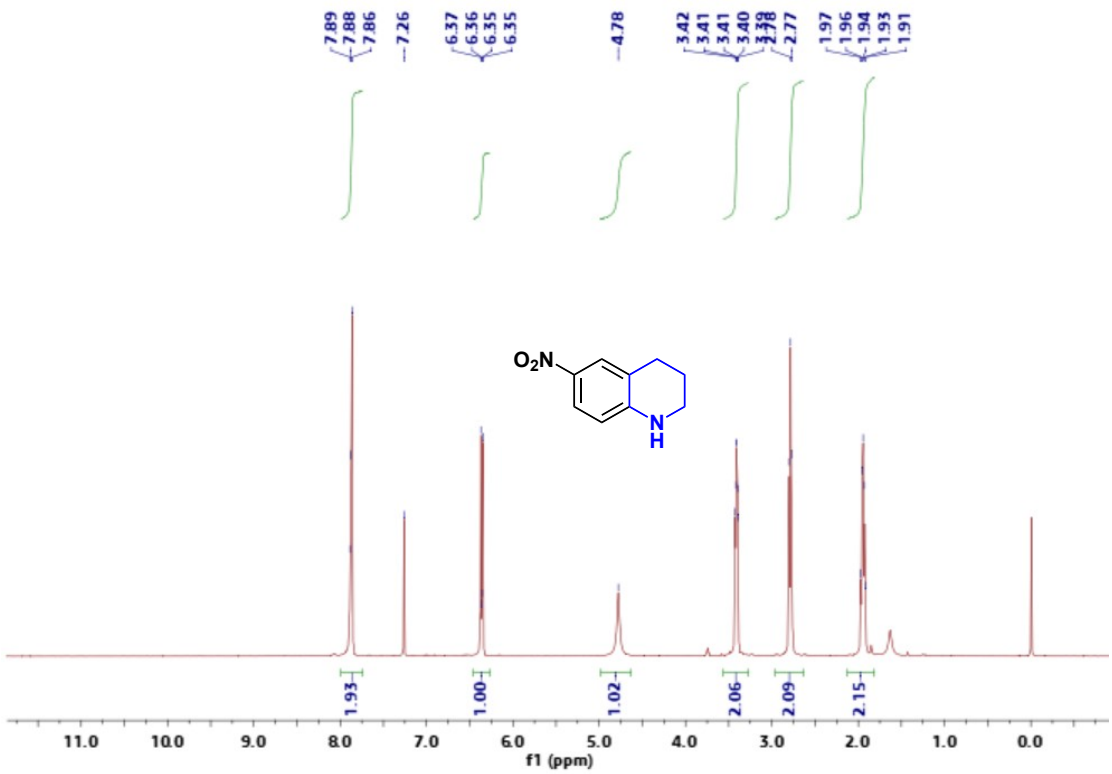
7.89
7.88
7.86
7.26
6.37
6.36
6.35
6.35
4.78
3.42
3.41
3.41
3.40
2.77
1.97
1.96
1.94
1.93
1.91
O2N
N
H
1.93
1.00
1.02
2.06
2.09
2.15
11.0
10.0
9.0
8.0
7.0
6.0
5.0
4.0
3.0
2.0
1.0
0.0
f1 (ppm)

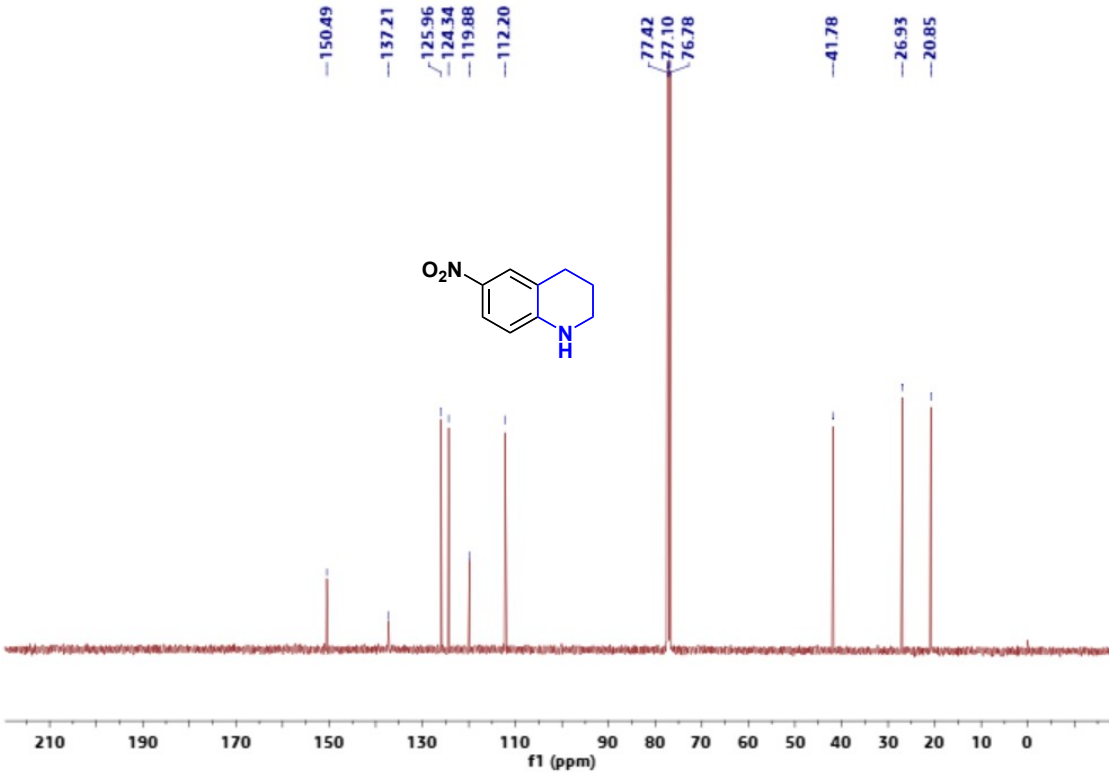
150.49
137.21
125.96
124.34
119.88
112.20
77.42
77.10
76.78
41.78
26.93
20.85
O2N
N
H
210
190
170
150
130
110
90
80
70
60
50
40
30
20
10
0
f1 (ppm)

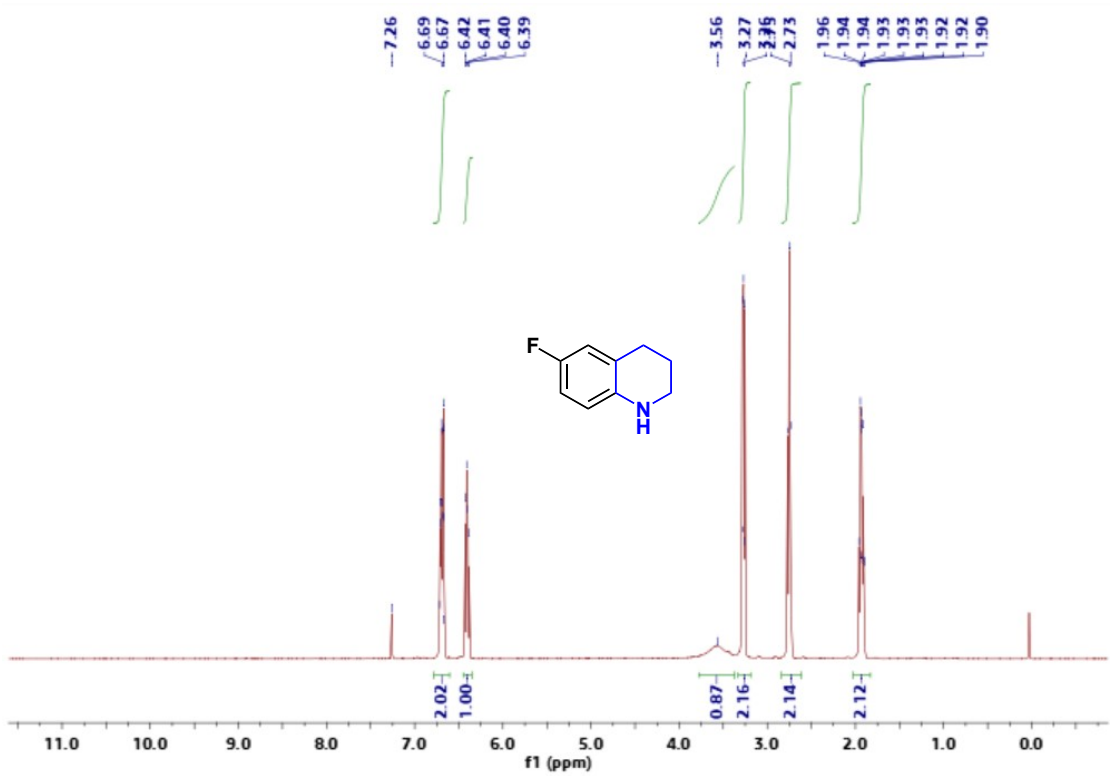
7.26
6.69
6.67
6.42
6.41
6.40
6.39
3.56
3.27
3.26
2.73
1.96
1.94
1.94
1.93
1.93
1.93
1.92
1.92
1.90
F
N
H
2.02
1.00
0.87
2.16
2.14
2.12
11.0
10.0
9.0
8.0
7.0
6.0
5.0
4.0
3.0
2.0
1.0
0.0
f1 (ppm)

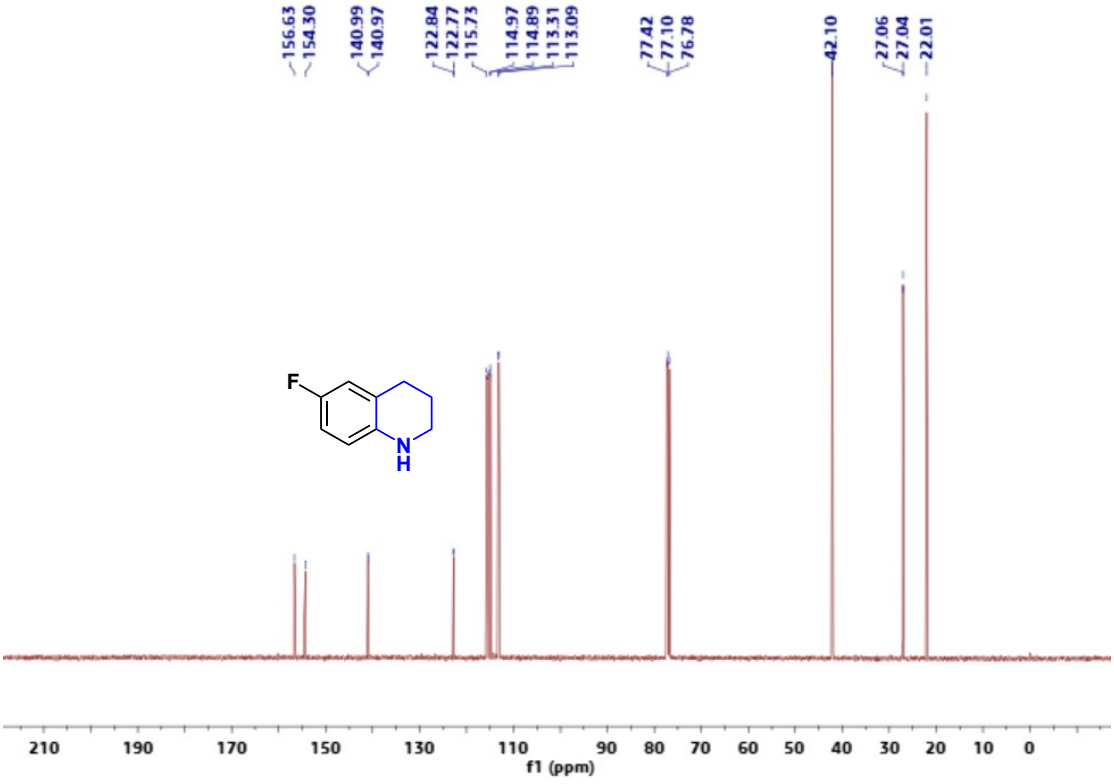
156.63
154.30
140.99
140.97
122.84
122.77
115.73
114.97
114.89
113.31
113.09
77.42
77.10
76.78
42.10
27.06
27.04
22.01
F
N
H
210
190
170
150
130
110
90
80
70
60
50
40
30
20
10
0
f1 (ppm)

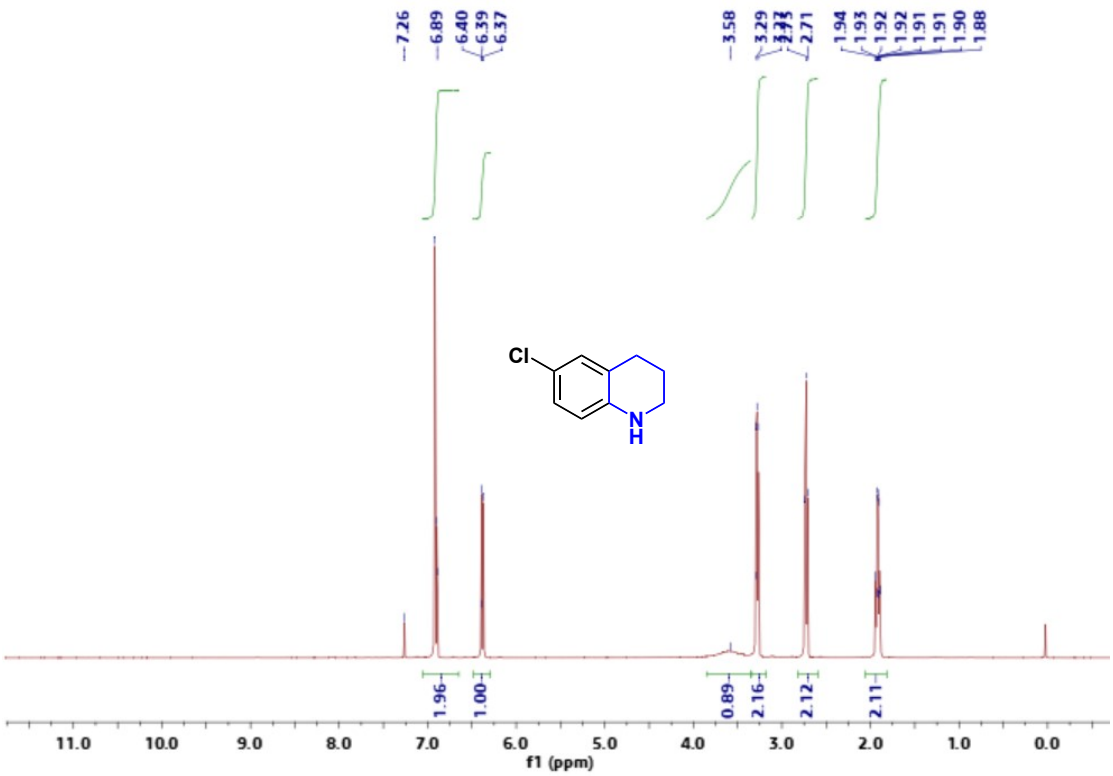
7.26
6.89
6.40
6.39
6.37
3.58
3.29
2.71
1.94
1.93
1.92
1.92
1.91
1.91
1.90
1.88
Cl
N
H
1.96
1.00
0.89
2.16
2.12
2.11
11.0
10.0
9.0
8.0
7.0
6.0
5.0
4.0
3.0
2.0
1.0
0.0
f1 (ppm)

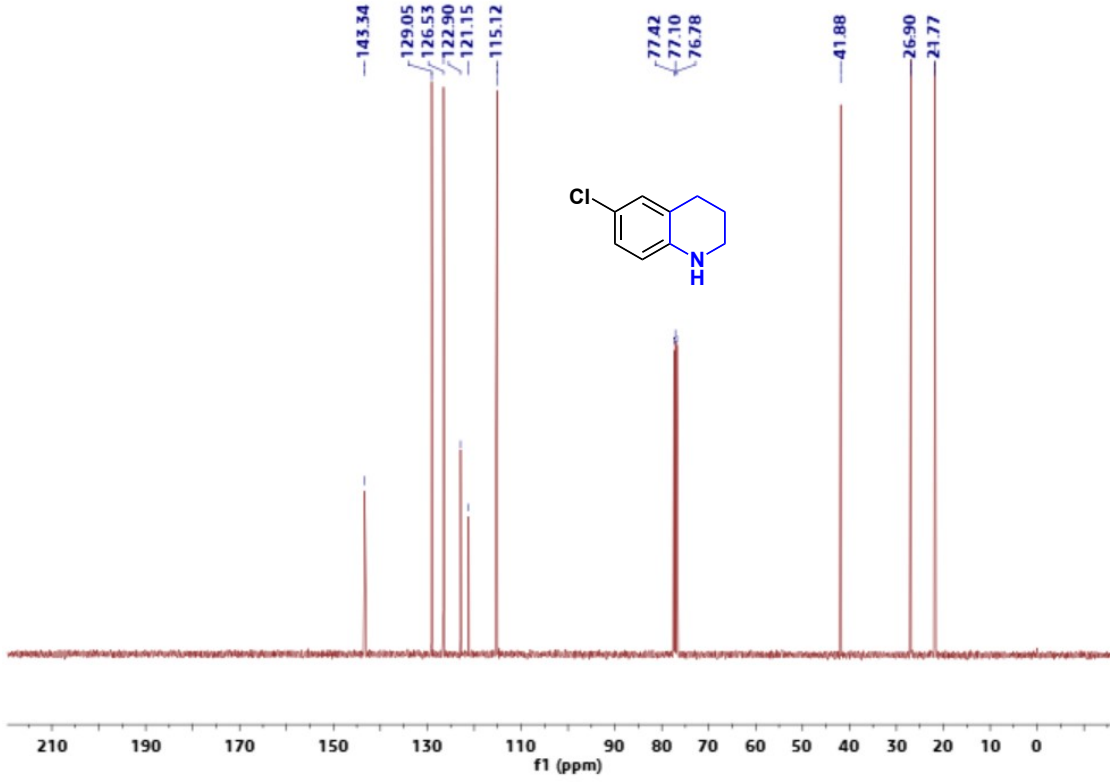
143.34
129.05
126.53
122.90
121.15
115.12
77.42
77.10
76.78
41.88
26.90
21.77
Cl
N
H
210
190
170
150
130
110
90
80
70
60
50
40
30
20
10
0
f1 (ppm)

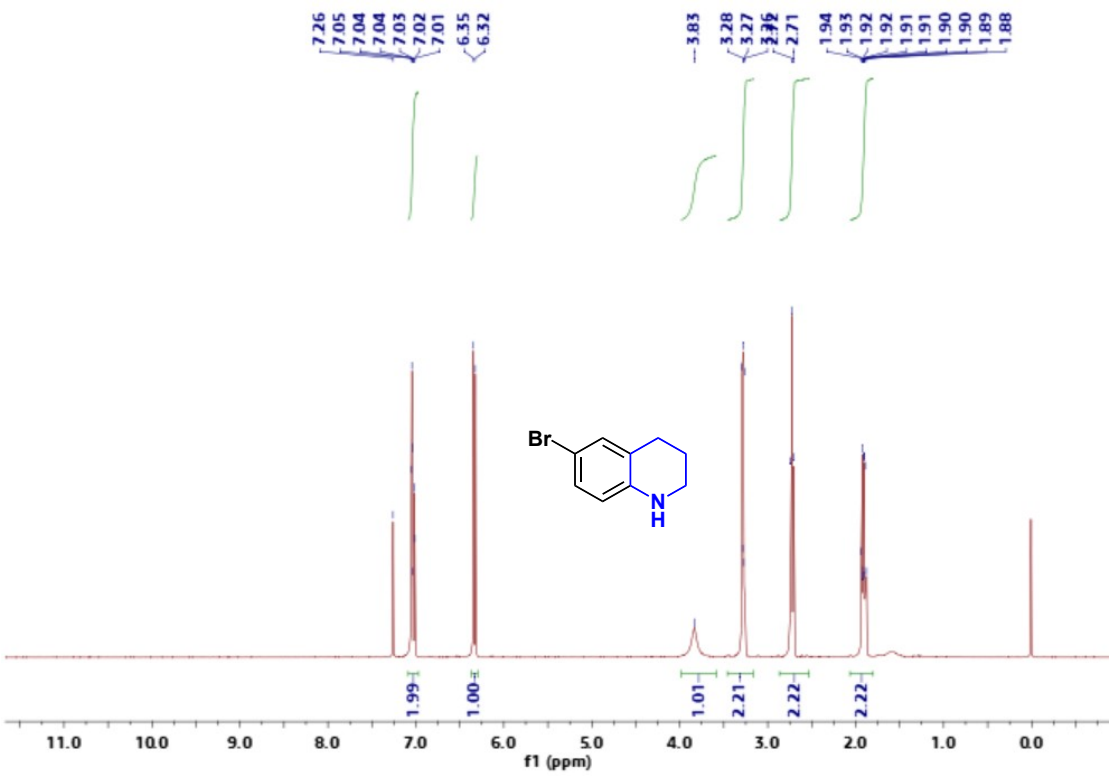
7.26
7.05
7.04
7.04
7.03
7.02
7.01
6.35
6.32
3.83
3.28
3.27
2.71
1.94
1.93
1.92
1.92
1.91
1.91
1.90
1.90
1.89
1.88
Br
N
H
1.99
1.00
1.01
2.21
2.22
2.22
11.0
10.0
9.0
8.0
7.0
6.0
5.0
4.0
3.0
2.0
1.0
0.0
f1 (ppm)

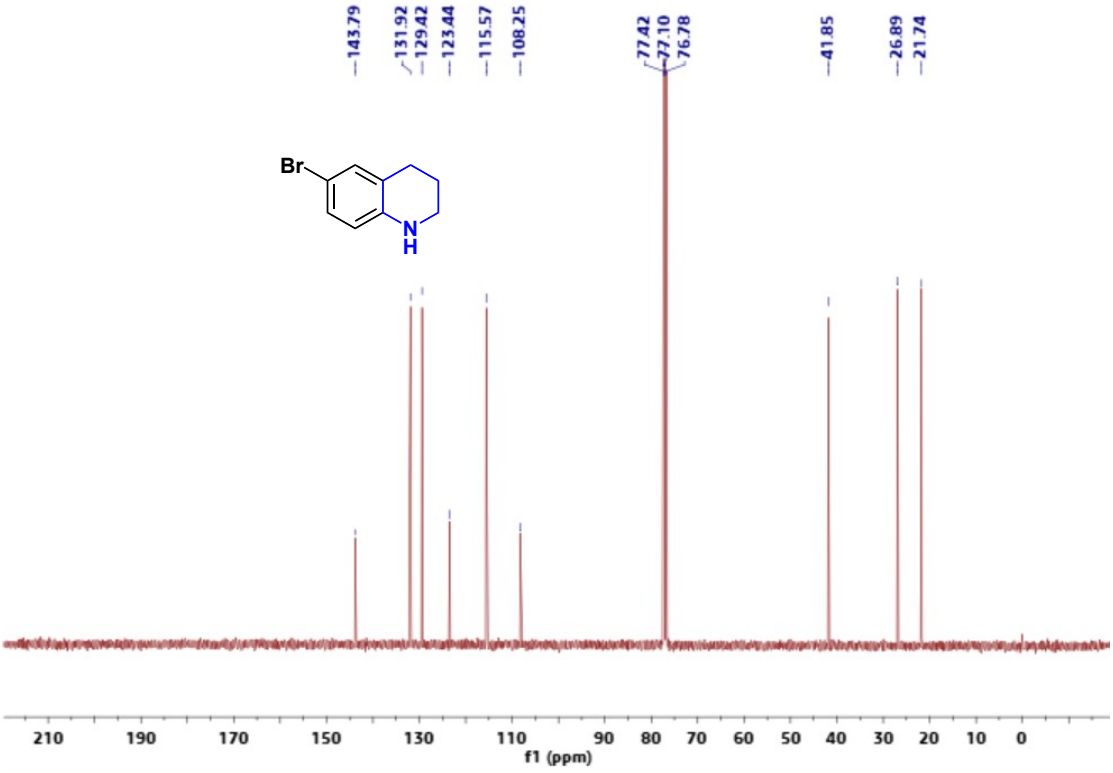
143.79
131.92
129.42
123.44
115.57
108.25
77.42
77.10
76.78
41.85
26.89
21.74
Br
N
H
210
190
170
150
130
110
90
80
70
60
50
40
30
20
10
0
f1 (ppm)

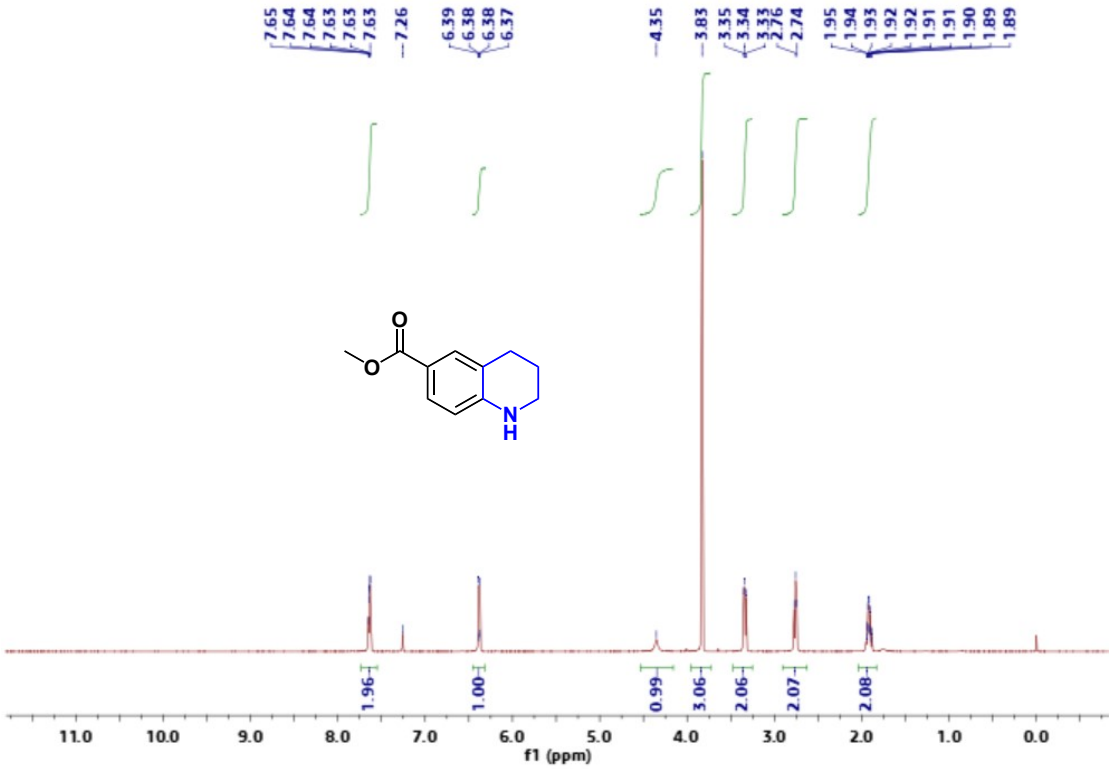
7.65
7.64
7.64
7.63
7.63
7.63
7.26
6.39
6.38
6.38
6.37
4.35
3.83
3.35
3.34
3.33
2.76
2.74
1.95
1.94
1.93
1.92
1.92
1.91
1.91
1.90
1.89
1.89
O
O
N
H
1.96
1.00
0.99
3.06
2.06
2.07
2.08
11.0
10.0
9.0
8.0
7.0
6.0
5.0
4.0
3.0
2.0
1.0
0.0
f1 (ppm)

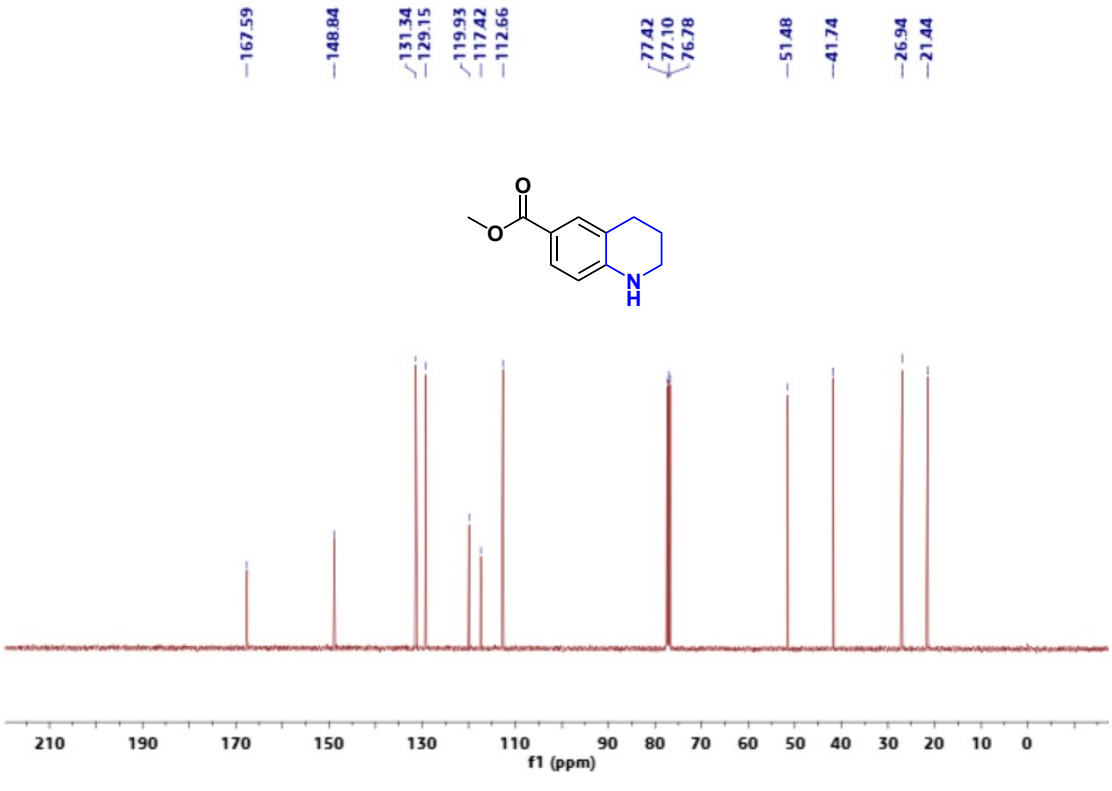
167.59
148.84
131.34
129.15
119.93
117.42
112.66
77.42
77.10
76.78
51.48
41.74
26.94
21.44
O
O
N
H
210
190
170
150
130
110
90
80
70
60
50
40
30
20
10
0
f1 (ppm)

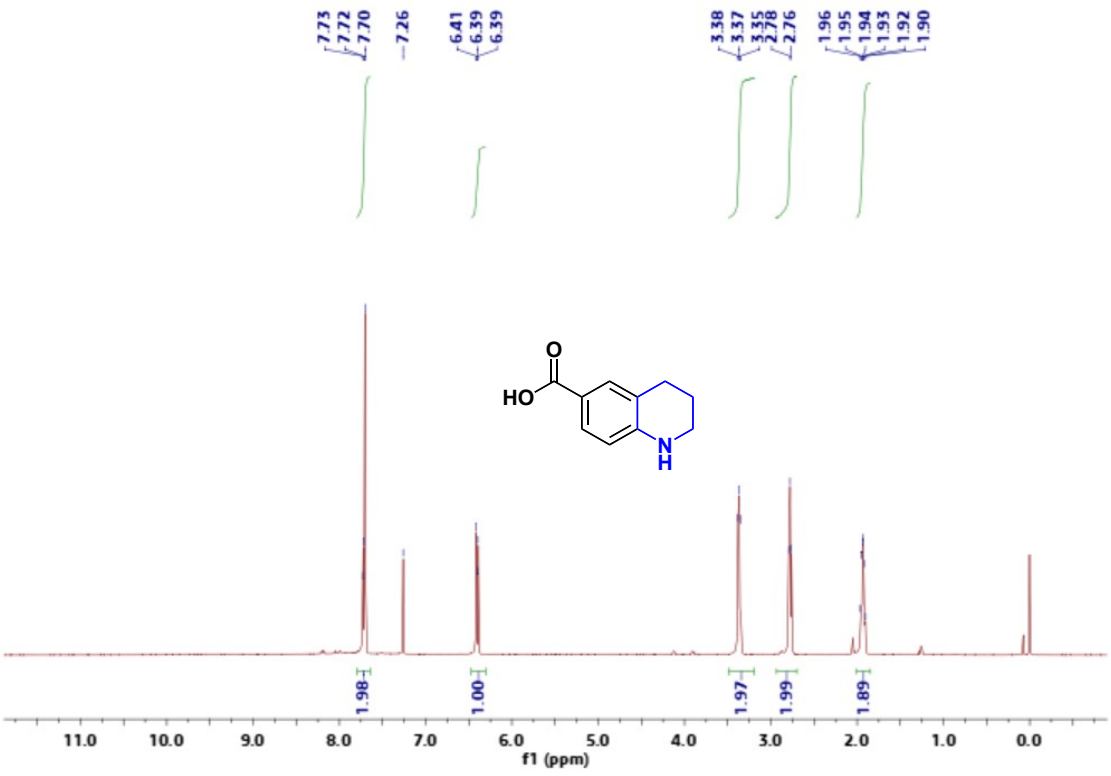
7.73
7.72
7.70
7.26
6.41
6.39
6.39
3.38
3.37
3.35
2.78
2.76
1.96
1.95
1.94
1.93
1.92
1.90
HO
O
N
H
1.98
1.00
1.97
1.99
1.89
11.0
10.0
9.0
8.0
7.0
6.0
5.0
4.0
3.0
2.0
1.0
0.0
f1 (ppm)

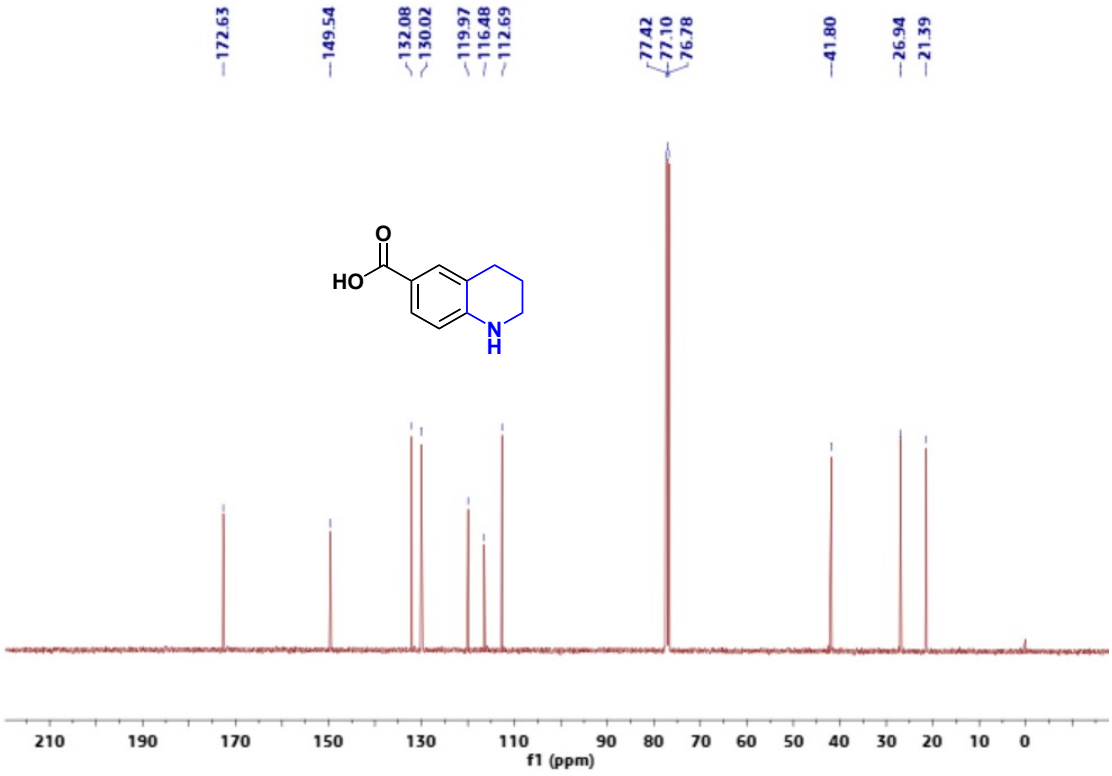
172.63
149.54
132.08
130.02
119.97
116.48
112.69
77.42
77.10
76.78
41.80
26.94
21.39
HO
O
N
H
210
190
170
150
130
110
90
80
70
60
50
40
30
20
10
0
f1 (ppm)

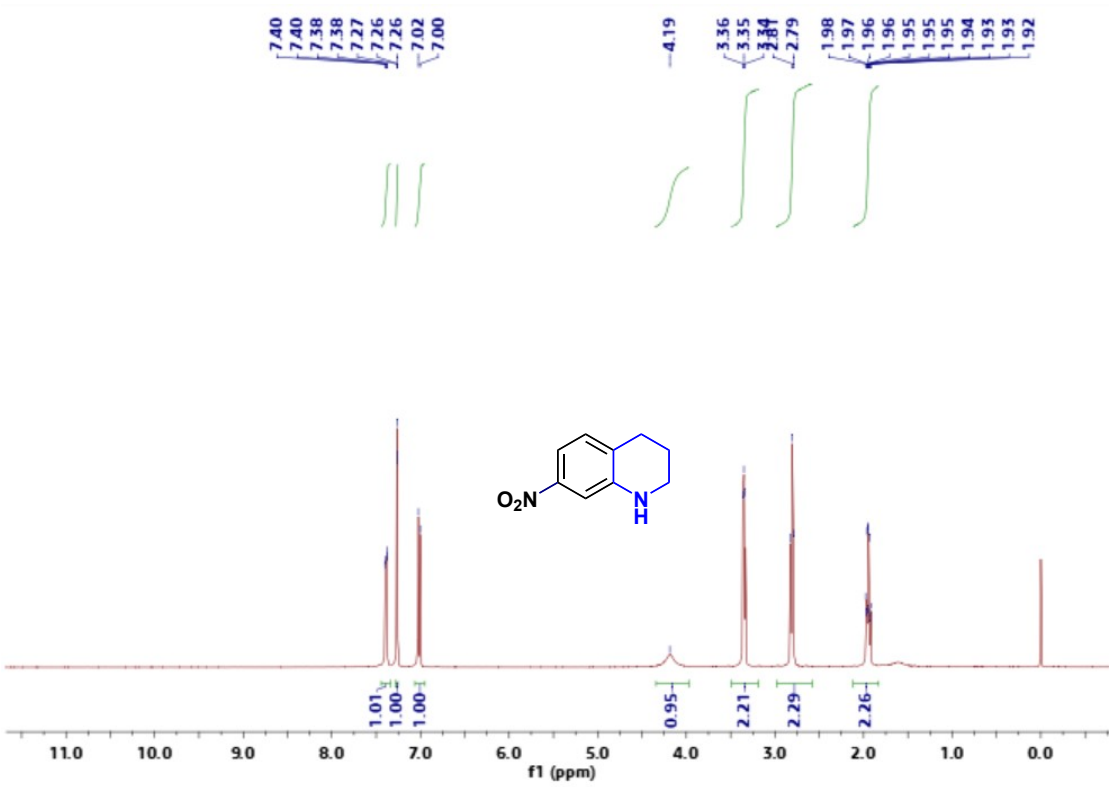
7.40
7.40
7.38
7.38
7.27
7.26
7.26
7.02
7.00
4.19
3.36
3.35
2.79
1.98
1.97
1.96
1.96
1.95
1.95
1.95
1.94
1.93
1.93
1.92
O2N
N
H
1.01
1.00
1.00
0.95
2.21
2.29
2.26
11.0
10.0
9.0
8.0
7.0
6.0
5.0
4.0
3.0
2.0
1.0
0.0
f1 (ppm)

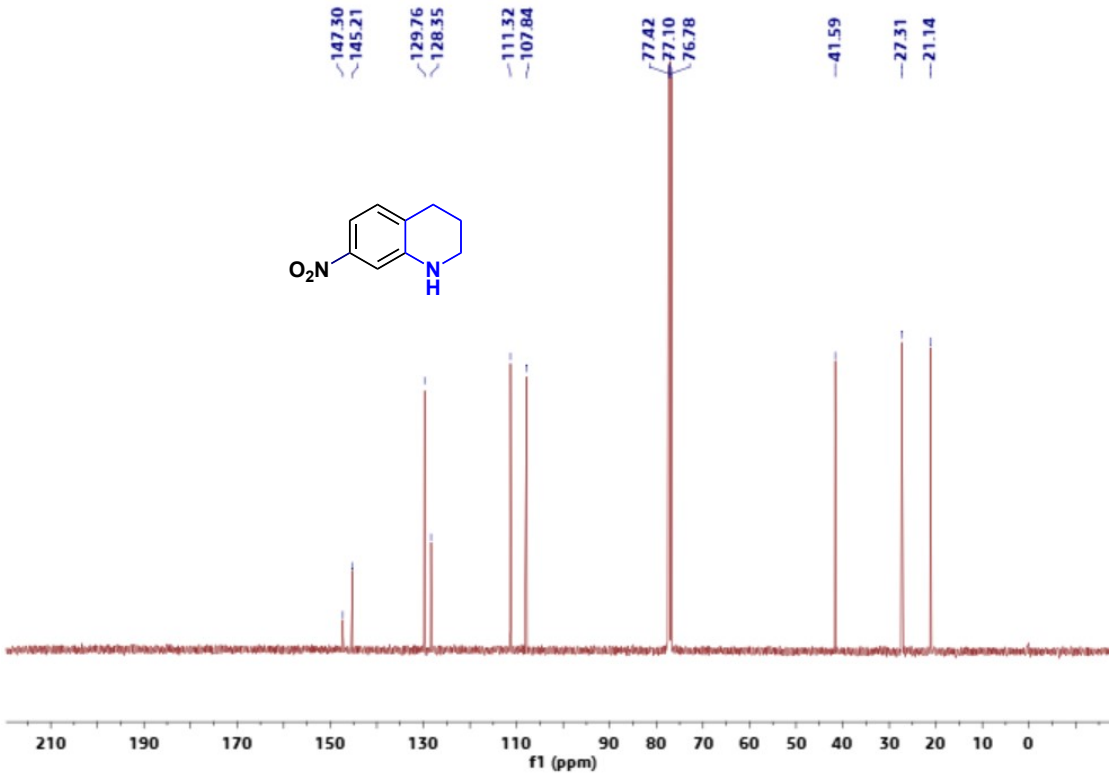
147.30
145.21
129.76
128.35
111.32
107.84
77.42
77.10
76.78
41.59
27.31
21.14
O2N
N
H
210
190
170
150
130
110
90
80
70
60
50
40
30
20
10
0
f1 (ppm)

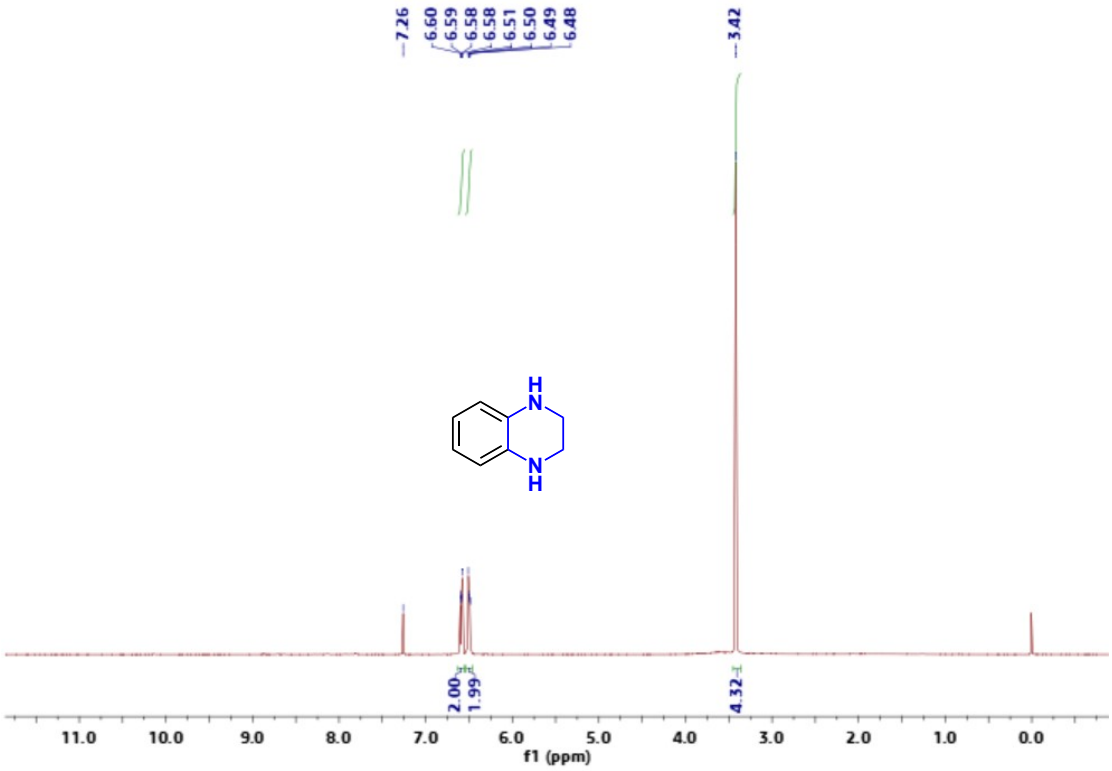
7.26
6.60
6.59
6.58
6.58
6.51
6.50
6.49
6.48
3.42
2.00
1.99
4.32
11.0
10.0
9.0
8.0
7.0
6.0
5.0
4.0
3.0
2.0
1.0
0.0
f1 (ppm)

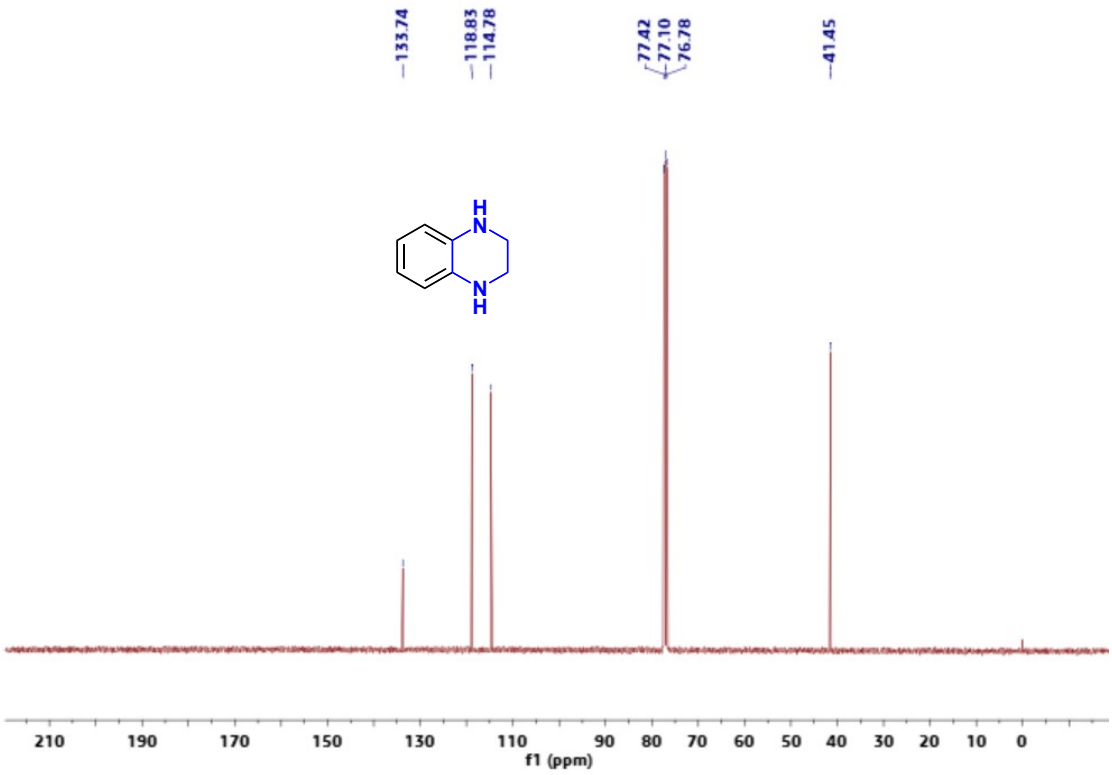
133.74
118.83
114.78
77.42
77.10
76.78
41.45
210
190
170
150
130
110
90
80
70
60
50
40
30
20
10
0
f1 (ppm)

Section G. Supporting References

[S1] C. R. Deblase, K. E. Silberstein, T. -T. Truong, H. D. Abruňa,W. R. Dichtel, *J. Am. Chem. Soc.* **2013**, *135*, 16821-16824.

[S2] M. Matsumoto, R. R. Dasari, W. Ji, C. H. Feriante, T. C. Parker, S. R. Marder, W. R. Dchtel, *J. Am. Chem. Soc.* **2017**, *139*, 4999-5002.

[S3]E. Vitaku, W. R. Dichtel, *J. Am. Chem. Soc.* **2017**, *139*, 12911-12914.